Research Article

Capsanthin/Capsorubin Synthase Expression in Tomato Alters Carotenoid Pools, Enhancing Provitamin A and Flavor Volatiles

Running title: Biofortifying tomato for provitamin A

Jingwei Fu[1], Denise Tieman[1], Bala Rathinasabapathi[1, *]

[1]Horticultural Sciences Department, University of Florida, Gainesville, FL 32611-0690

*Corresponding author E-mail: brath@ufl.edu

Word count: 8013 words
Number of figures: 10
Number of tables: 0
Supporting information:
Supplementary figures: 10
Supplementary tables: 3
Supplementary data file: 1

20 **One sentence summary**
21
22 Expression of capsanthin/capsorubin synthase in tomato enhanced total carotenoids, β-carotene,
23 ketocarotenoids and flavor volatiles in ripening fruit with no impact on plant growth and
24 development.

Abstract

We conceptualized a tomato biofortification strategy via engineering simultaneous accumulation of *β*-carotene, a provitamin A and pepper-specialized ketocarotenoids, capsanthin, and capsorubin. Capsanthin/capsorubin synthase (CCS) in pepper, an enzyme phylogenetically related to lycopene β-cyclases (LCYB) known for *β*-carotene synthesis, was investigated for its *in vivo* role in ripening fruit. In pepper, silencing of *CCS* via virus-induced gene silencing reduced the flux from lycopene to *β*-carotene (the *β*-branch) with significant changes in carotenoid compositions. In a carotenogenic bacterial expression system, pepper CCS was more effective than tomato LCYB1 or LCYB2 in lycopene cyclization to *β*-carotene and CCS synthesized capsanthin, but the LCYBs did not. Therefore, we overexpressed pepper *CCS* in different tomato varieties, including 'Micro-Tom' WT, 'Micro-Tom' mutant, *pyp1-1(H7L)* (defective in xanthophyll esterification), and five inbreds and characterized their carotenoid profiles. In *CCS*-transformed tomato fruit (WT and selected varieties), besides the biosynthesis of capsanthin and capsorubin, total carotenoids, *β*-carotene, and xanthophyll esters remarkably increased compared to the controls, while such increments were weaker in the *pyp1-1(H7L)*. CCS expression had a positive influence on the flux toward the *β*-branch and the storage pool of xanthophyll esters consistent with its dual functions in lycopene cyclization and ketocarotenoid biosynthesis. The data further supported that xanthophyll esters facilitated carotenoid accumulation. While CCS-expression had no significant impact on growth or yield, fruit of *CCS*-transformed tomato had greater levels of *β*-carotene-derived flavor volatiles than the controls. Consumption of 37–131-gram of *CCS*-derived hybrid fruit meets the provitamin A recommended dietary allowance, indicating greatly improved nutritional value.

Keywords: Beta-carotene, Capsanthin, Carotenoid, Metabolic engineering, *Solanum lycopersicum*, Synthetic biology, Xanthophyll esters, *Escherichia coli*

52 **Introduction**

53 Pepper fruit, a nutrient-dense vegetable for human consumption, contains health-
54 promoting metabolites, including vitamins, alkaloids, and specialized metabolites such as
55 capsanthin, and capsorubin (Wahyuni *et al.*, 2013). Capsanthin and capsorubin are
56 ketocarotenoids, accumulating in the ripe fruit of *Capsicum* and a few other taxa (Trajković *et*
57 *al.*, 2021). Capsanthin/capsorubin synthase (CCS, EC no.: 5.3.99.8) is responsible for the
58 biosynthesis of capsanthin and capsorubin using antheraxanthin and violaxanthin as substrates,
59 respectively (Bouvier *et al.*, 1994; Mialoundama *et al.*, 2010). CCS was first identified from
60 pepper (Bouvier *et al.*, 1994), and validated through enzymatic assays *in vitro* (Mialoundama *et*
61 *al.*, 2010). In addition to *k*-cyclase activity, CCS was reported to have the catalytic activity of
62 lycopene beta-cyclase (LCYB) also, via *in vitro* assays converting lycopene into *β*-carotene
63 (Cunningham *et al.*, 1994; Bouvier *et al.*, 1997; Mialoundama *et al.*, 2010). In pepper fruit, the
64 majority of capsanthin and capsorubin are esterified by a xanthophyll acyltransferase (XAT) and
65 stored inside the plastoglobule (Berry *et al.*, 2019). The xanthophyll esterification to fatty acyl
66 groups improves their accumulation, stability, and storage (Ariizumi *et al.*, 2014; Li *et al.*, 2023).
67 However, the relationship between the biosynthesis of abundant ketocarotenoids and the process
68 of xanthophyll esterification in pepper fruit is still unclear. The *in vivo* role of CCS in the
69 carotenoid pool of ripe pepper fruit remains poorly understood as well, although CCS was well
70 known to have lycopene cyclase and *k*-cyclase activities and be associated with xanthophyll
71 esterification process. We hypothesized that transferring *CCS* from pepper to other related plant
72 species could allow us to test its role in carotenoid biosynthetic flux and accumulation, and the
73 production of specialized ketocarotenoids, and their esters. To date, stable genetic transformation
74 of plants expressing *CCS* in the endosperm of rice (Ha *et al.*, 2019) and in the flower of *Viola*
75 *cornuta* (Trajković *et al.*, 2021) have been reported. However, the alteration of the carotenoid
76 pathway by CCS in a fleshy fruit has remained elusive.

77 Metabolic engineering is an efficient method to biofortify crops in a targeted direction
78 (Van Der Straeten *et al.*, 2020), such as purple tomato engineered to accumulate anthocyanins
79 (Butelli *et al.*, 2008). Vitamin A is indispensable for human health since vitamin A deficiency
80 (VAD) may result in the development of disorders like xerophthalmia, blindness, and anemia
81 (Blaner, 2020). Globally, an estimated 250–500 million preschool children suffer from VAD
82 (World Health Organization). Hence, carotenoid biofortification of nutrient-dense plant-based

83 foods is an excellent approach to simultaneously combat food insecurity and VAD (Kraemer *et*
84 *al.*, 2008; Grune *et al.*, 2010; Fitzpatrick *et al.*, 2012; Blaner, 2020).
85 Multiple cases of carotenoid pathway engineering have been performed to biofortify
86 crops with *β*-carotene, the major provitamin A (Giuliano, 2017; Zheng *et al.*, 2020), including the
87 first example, golden rice, in which *β*-carotene accumulated in rice endosperm (Ye & Beyer,
88 2000). In addition to provitamin A, the alteration of non-provitamin A carotenoids, like lycopene,
89 lutein, and zeaxanthin, through metabolic engineering is also of interest. The pepper
90 ketocarotenoids, capsanthin and capsorubin, are reported to have higher antioxidant ability and
91 potential health promoting activities tested by cell culture and animal model studies (Nishino *et*
92 *al.*, 2016; Kennedy *et al.*, 2021). Besides crops, carotenoid metabolic engineering has been
93 fulfilled in microbes, especially in *E. coli* (Lee & Schmidt-Dannert, 2002; Furubayashi *et al.*,
94 2021; Xu *et al.*, 2023).
95 Hence, we aimed to (1) test the *in vivo* role of CCS in carotenoid pools of pepper fruit,
96 (2) compare enzymatic function of pepper CCS and tomato LCYBs, and (3) test the impact of
97 CCS overexpression and xanthophyll esterification in tomato fruit potentially increasing the
98 levels of total carotenoids, provitamin A carotenoid *β*-carotene, volatile apocarotenoids and
99 ketocarotenoids capsanthin and capsorubin. Taking advantage of multiple functions of CCS, we
100 overexpressed pepper *CCS* in 'Micro-Tom' WT and a 'Micro-Tom' mutant, *pyp1-1(H7L)*,
101 defective in xanthophyll esterification (Ariizumi *et al.*, 2014). CCS altered the compositions and
102 the flux in the carotenoid pathway of *CCS*-transformed tomato fruit, resulting in higher
103 accumulation of total carotenoids, *β*-carotene, and xanthophyll esters. The results from
104 overexpressing *CCS* in the mutant background indicated that xanthophyll esterification process is
105 important for carotenoid biosynthesis and accumulation. Furthermore, we introduced *CCS* into
106 five different tomato inbreds through controlled crosses, which resulted in remarkable
107 improvements of *β*-carotene levels. CCS-overexpression also increased volatile apocarotenoids
108 derived from β-carotene with no significant impact on plant growth and yield. We demonstrated
109 that the tomato fruit biofortified with high provitamin A and ketocarotenoids would be an
110 excellent dietary source for human nutrition and to address VAD.

111 **Materials and Methods**

112 **Plant materials and growth conditions**

113 Seeds of wild-type (WT) *Solanum lycopersicum* L. cv Micro-Tom, and *pale yellow petal*
114 *1-1* mutant (*pyp1-1*, TOMJPE-H7L, Fig. S1) in 'Micro-Tom' background, were from
115 TOMATOMA, Japan (Saito *et al.*, 2011). The mutant *pyp1-1* exhibits an inability to synthesize
116 xanthophyll esters (Ariizumi *et al.*, 2014). Seeds of LA2374 ('Caro Red'), LA2377 ('Purple
117 Calabash'), and LA4044 (*Solanum pennellii*, IL3-2, (Alseekh *et al.*, 2013) were from the Tomato
118 Genetics Resource Center (University of California, Davis, CA, U.S.A.). Seeds of FL7907B
119 were from Dr. S.Hutton (GCREC, University of Florida, Wimauma, FL, U.S.A.). Seeds of 'Jaune
120 Flamme' were from Tomato Grower's Supply Company (Fort Myers, FL, U.S.A.). Seedlings
121 were grown in a potting medium (Jolly Gardener, C25) supplied with controlled-release fertilizer
122 (Florikan, N: K:P=18:6:8). Growing conditions were as follows: 16-h-day/8-h-night photoperiod,
123 25ºC/22ºC day/night temperature, 50% relative humidity, and ~150 μmol m^{-2} s^{-1} light intensity
124 supplemented by fluorescent lights.

125 **cDNA Cloning**

126 Total RNA was isolated from ripe pepper pericarp of RJ107(6)A3 (Maquilan *et al.*, 2020)
127 using RNeasy plant mini kit (Qiagen, Germany). First-strand cDNA was synthesized using
128 SuperScript®III First-Strand Synthesis System (Invitrogen, U.S.A.). Capsanthin/capsorubin
129 synthase (CCS, Capana06g000615, PP418871.1) protein coding sequence (CDS) minus stop
130 codon were amplified from first strand cDNA using specific primers listed in Table S1. The gel-
131 purified amplicons were cloned into an entry vector pENTR™/D-TOPO® (Invitrogen, U.S.A.).
132 *CaCCS* cDNA from the entry vector were subcloned into plant expression vector pK7FWG2.0
133 by Gateway LR recombination reaction (Invitrogen, U.S.A.) to generate pK7FWG2.0-CaCCS-
134 eGFP. Following all cloning operations, sequence verification was done by Sanger sequencing.

135 **Virus-Induced *ccs*-Silencing in Pepper Fruit**

136 The *CCS* knock-down pepper lines were generated by the VIGS modified from (Liu *et*
137 *al.*, 2002). The target region for silencing was designed by the SGN VIGS Tool
138 (https://vigs.solgenomics.net). The output suggested the best target region and no potential off-
139 target in that 460 bp fragment of *CaCCS*. It was amplified from pepper fruit cDNA using specific
140 primers listed in Table S1. After subcloning into pTRV2-MCS, which was obtained along with
141 pTRV1 from the Arabidopsis Biological Resource Center, pTRV2-CCS was generated. This

142 plasmid was transformed into *Agrobacterium tumefaciens* strain GV3101. The agroinfiltration of
143 pepper plants was performed as previously described (Kim *et al.*, 2017). *Agrobacterium* strains
144 GV3101 harboring pTRV2-CCS and pTRV1 were mixed 1:1 and infiltrated onto open cotyledons
145 using 1-mL syringe without needles. The *Agrobacterium* strain GV3101 containing pTRV2-MCS
146 was used as a control. Infiltrated plants were kept under dark and high humidity conditions
147 overnight, followed by normal conditions.

148 **Quantitative Real-Time PCR**

149 RNA extraction and single-stranded cDNA were prepared as described in 'cDNA
150 Cloning'. The expression level of *CCS* gene was estimated by quantitative RT-PCR using green
151 fast qPCR blue mix (AzuraView^{TM}, MA, U.S.A.) with gene-specific primers (Table S1). The
152 relative expression levels of targeted genes were quantified using the equation of $2^{\wedge-\Delta CT}$,
153 normalized to the gene encoding ubiquitin-conjugating enzyme E2 (Cheng *et al.*, 2017). Each
154 qPCR reaction was run in four biological and three technical replicates.

155 **Plasmid Construction and Carotenoid Production in *E. coli***

156 Background plasmids, pAC-LYCipi (plasmid # 53279) and pAC-VIOL (Plasmid
157 #53087), were obtained from Addgene, which was developed previously to produce lycopene
158 and violaxanthin, respectively, in *Escherichia coli* (Cunningham *et al.*, 2007; Neuman *et al.*,
159 2014). The background plasmid was transformed into an *E. coli* strain, SixPack, derived from
160 BL21(DE3) (Lipinszki *et al.*, 2018). Pepper and tomato cDNAs were prepared as described in
161 'cDNA Cloning'. The cDNA of CaCCS, SlLYCB1 (Solyc04g040190), and SlLCYB2
162 (Solyc10g079480) minus transient peptide sequence was amplified using specific primers listed
163 in Tab. S1. After subcloning into pET30a (Novagen), pET30-CaCCS, pET30-SlLCYB1 and
164 pET30-SlLCYB2 were generated, sequenced, and used for *E. coli* transformation.

165 pET30a plasmids, including empty vector (pET30a), pET30-CaCCS, pET30-SlLCYB1,
166 and pET30-SlLCYB2, were transformed into chemically competent SixPack cells harboring the
167 background plasmid encoding carotenoid biosynthetic genes (pAC-LYCipi or pAC-VIOL).
168 Three individual colonies for each transformation were picked and validated through colony
169 PCR. After validation, they were inoculated separately in 10-mL LB liquid media containing 30
170 mg L^{-1} of chloramphenicol and 50 mg L^{-1} of kanamycin. The starter cultures were grown at
171 37 °C until saturation. In the following day, 1 ml of overnight culture was used to inoculate 100
172 ml of Terrific Broth (TB) medium containing 30 mg L^{-1} of chloramphenicol and 50 mg L^{-1} of

173 kanamycin in a 250-ml Erlenmeyer flask. The cultures were grown at 200 rpm at 37 °C until an
174 absorbance at 600 nm of 1.0 was achieved. The cells were chilled on ice for 10 min and induced
175 with a final concentration of 0.1 mM isopropyl *β*-D-1-thiogalactopyranoside (IPTG). The
176 cultures were returned to the shaker and grown for 24 h at 200 rpm at 16ºC in the darkness.
177 Then, the cultures were shaken at 25ºC for an additional 60 h at 200 rpm in the darkness. The
178 cells were harvested by high-speed centrifugation, which were used for the extraction and
179 chromatographic analysis of carotenoids.

180 **Plant transformation**

181 *Agrobacterium*-mediated transformation of tomato was performed using the method of
182 Sun et al., (2006) with modifications. *Agrobacterium* GV3101 harboring pK7FWG2.0-CaCCS-
183 eGFP were grown in YEP to prepare *Agrobacterium* inoculum. Surface-sterilized seeds of WT
184 'Micro-Tom' and *pyp1-1* mutant were germinated on half-strength MS medium (Murashige &
185 Skoog, 1962). Cotyledon explants from 10-day old seedlings were placed on a preculture
186 medium for 48h, blotted dry and placed on a co-cultivation medium at 25ºC in the dark for 48h.
187 Subsequently, the explants were transferred to the callus induction medium for two weeks and
188 then to shoot induction medium until shoots formed. Elongated shoots were excised and
189 transferred to the rooting medium. Rooted shoots were transplanted to soil. Media components
190 are listed in Table S2. Genomic PCR with T-DNA-specific primers combining flower
191 phenotyping was performed to identify the putative transformants. More than a hundred of T_0
192 plants were screened (257 for WTCCS and 163 for CCS). Validated T_0 transgenic lines were
193 grown to collect seeds, from which representative WTCCS transgenic lines and CCS transgenic
194 lines at T_2 generation were used for further analyses.

195 The transgene copy numbers were evaluated using qPCR and serial dilution of genomic
196 DNA against systemin and phytoene desaturase genes in the genome as the endogenous
197 references (Chetty *et al.*, 2013; Kanwar *et al.*, 2022). Data on representative transgenic lines
198 presented in Figures 2 to 8 have been verified to contain a single copy of CCS integrated into
199 their genomes. Data on additional transgenic lines are presented in Figures S8 and S9.

200 **Control- and *CCS*-derived tomato lines**

201 Five tomato inbreds, 'FL7907B', 'LA2377', 'LA2374', 'Jaune Flamme', and 'LA4044',
202 were selected as maternal lines. The transgenic lines, WTCCS46 and WTCCS59 generated in
203 this study and 'Micro-Tom' (WT background) were used as paternal lines. Pollen from the

204 WTCCS46 or WTCCS59 was transferred onto the stigma of emasculated flowers of the selected
205 lines, to generate *CCS*-derived lines. Similar crosses were made between WT 'Micro-Tom' and
206 the selected lines to generate control-derived lines. Seeds of ripe fruit resulting from crosses
207 were collected and germinated to generate the F1 plants. Ten plants from each cross were grown
208 as biological replicates. All F1 plants harboring the transgene were validated by genomic PCR
209 with T-DNA-specific primers (Tab. S1). The F1 plants were grown in a temperature-controlled
210 greenhouse in 5-gallon containers filled with potting medium and fertilized with the Tomato
211 Plant Food (MiracleGro, Marysville, OH, U.S.A.) every week. The ripe fruit from all lines were
212 collected for analyses.

213 **Carotenoid analysis**

214 Carotenoids were extracted from pepper or tomato pericarp, or *E coli* cells following the
215 method of Wahyuni (2011). The pooled organic solvent layers from extracts were combined,
216 dried under a nitrogen stream, and were used either for direct quantification (unsaponified) or for
217 saponification based on the method of Mínguez-Mosquera & Hornero-Méndez (1993).
218 Quantification of carotenoids was performed by HPLC-UV/Vis following the method adapted
219 from Delgado-Pelayo & Hornero-Méndez (2012). The chromatographic system comprised an
220 Agilent 1100 chromatograph connected to an Agilent G1314A UV/Vis detector operated by
221 ChemStation software. The chromatographic conditions are listed in Table S3. Lycopene and *β*-
222 carotene standards were from Sigma-Aldrich (MO, U.S.A.). Zeaxanthin, lutein, and zeaxanthin
223 dipalmitate were from Cayman. Capsanthin and capsorubin were purified from pepper fruit by
224 column chromatography using the methods of Cvetković & Marković (2008). Each carotenoid
225 concentration was calculated using the standard curves. The xanthophyll ester fractions were
226 quantified using the calibration curve of zeaxanthin dipalmitate since standards for most other
227 xanthophyll esters were not commercially accessible. Concentration was calculated as μg per
228 gram of fresh weight (μg g^{-1} f.wt.).

229 **Analysis of flavor volatiles from ripe fruit**

230 Freshly harvested ripe fruit from greenhouse-grown control and *CCS*-derived hybrids
231 were used to quantify volatile apocarotenoids (Tieman *et al.*, 2006). Briefly, a 100 g sample of
232 chopped fruit was placed inside a glass tube through which air filtered through a hydrocarbon
233 trap (Agilent, Palo Alto, CA) was flowing through for 1 h. The volatile apocarotenoids were
234 collected on a Super Q column, which was then eluted with methylene chloride after the addition

of nonyl acetate as an internal standard. VOC were separated on an Agilent (Palo Alto, CA) DB-5 column and analyzed using an Agilent 6890N gas chromatograph. Compounds were identified based on retention times compared to standard compounds (Sigma Aldrich, St Louis, MO). The volatile amounts were computed based on peak areas calibrated by internal standards and expressed as ng^{-1} $gfwt^{-1}$ h^{-1}.

240 **Results**

241 **Characterization of capsanthin/capsorubin synthase (CCS) in pepper carotenoid pathway**

242 A Pearson correlation analysis on the relationship between the contents of paired
243 carotenoids from 32 pepper varieties adopted from a previous study (Wahyuni *et al.*, 2011)
244 showed that capsanthin and capsorubin contents were positively correlated with *β*-carotene
245 contents (r=0.88) (Fig. S2), suggesting a role for CCS in accumulation of capsanthin, capsorubin,
246 and *β*-carotene in pepper fruit. To confirm CCS' function in the carotenoid pathway, *CCS*
247 expression in pepper fruit was silenced through virus-induced gene silencing (VIGS). The
248 relative expression of the *CCS* transcript dropped >10-fold in *ccs*-silenced fruit compared to the
249 mock, paralleling with the yellow color of ripe fruit as opposed to the red of the mock control
250 (Fig. 1a). The carotenoid profile of *ccs*-silenced fruit showed a distinguishable difference from
251 that of mock-treated fruit (Fig. 1b). Compared to mock-treated fruit, total carotenoids were
252 significantly reduced in the *ccs*-silenced fruit, among which xanthophyll esters and carotenes
253 decreased by 61.5% and 37.4% respectively (Fig. 1c, f). Specifically, lutein and *α*-carotene
254 contents in the *α*-branch of the carotenoid pathway were elevated by 13.2 and 1.6-fold
255 respectively when *CCS* expression was silenced (Fig. 1d, f). Oppositely, capsanthin and
256 capsorubin levels in the *β*-branch were reduced by 96% and 99% respectively in *ccs*-silenced
257 fruit (Fig. 1f). The silencing of the *CCS* gene in pepper fruit reduced not only capsanthin and
258 capsorubin, but also *β*-carotene levels by 46% in pepper fruit (Fig. 1e, f), consistent with the
259 results of correlation analysis. In the *β*-branch, the amounts of other carotenoids, except for (*all*
260 *E*) violaxanthin and (*9'Z*) violaxanthin, were reduced significantly as well in *ccs*-silenced fruit
261 (Fig. 1e, f).

262 **Functional validation and comparison of pepper CCS and tomato LCYBs**

263 To compare the enzymatic function of pepper CCS and tomato LCYBs, they were
264 heterologously expressed in an *E. coli* system, respectively (Fig. 2). First, we tested their
265 lycopene cyclase activity in *vivo* (Fig. 2a). The *E. coli* cells accumulated 133.9 μg g^{-1} f.wt. cells
266 of lycopene when it harbored the background plasmid, pAC-LYCipi, and empty vector, pET30a
267 (Fig. 2b&c). When the additional CCS or LCYBs were expressed along with pAC-LYCipi, *β*-
268 carotene was detected in *E. coli* cells (Fig. 2b–d). Specifically, pepper CCS harboring cells
269 accumulated 158.0 μg g^{-1} f.wt. cells of *β*-carotene, accounting for 96% of total carotenoids (Fig.
270 2b–d). However, both tomato LCYBs harboring cells accumulated 31.7~37.0 μg g^{-1} f.wt. cells of

271 *β*-carotene and 48.5 and 63.4 μg g^{-1} f.wt. cells of lycopene remaining in *E coli* cells (Fig. 2b–d).
272 Subsequently, to further test the unique function of CCS in ketocarotenoid biosynthesis, another
273 background plasmid, pAC-VIOL, was transformed in *E. coli* to produce precursors,
274 antheraxanthin or violaxanthin (Fig. 2e). The *E. coli* harboring pAC-VIOL along with the empty
275 vector accumulated small amounts of xanthophylls including violaxanthin, antheraxanthin and
276 zeaxanthin (Fig. 2f). However, when CCS or LCYBs were expressed with pAC-VIOL, the total
277 carotenoids were increased (Fig.2f). The substrate, antheraxanthin, for ketocarotenoid synthesis
278 was increased 1.1 to 1.6-fold in LCYBs harboring *E. coli*, while it remained at similar level in
279 CCS harboring *E. coli* (Fig. 2g). Accordingly, capsanthin was detected in CCS harboring *E. coli*
280 but not in LCYBs harboring *E. coli* (Fig. 2h).

281 **Phenotypic alteration of *CCS*-overexpression tomato lines**

282 In a control tomato WTEV21 (wildtype background transformed with empty vector,
283 line21) and 1-1EV11 (*pyp1-1(H7L)* background transformed with empty vector, line11), ripe
284 fruit remained red comparable to WT and *pyp1-1(H7L)*, showing no visible differences generated
285 by the empty vector (Fig. 3a, e). When tomato was engineered for constitutive expression of
286 pepper *CCS*, no obvious difference in plant growth and yield was observed, compared to the
287 control lines (Fig. S3). However, the ripe fruit color changed from red to red-orange (WTCCS46
288 line, a representative line of wildtype background transformed with *CCS*, Fig. 3a). In mutant
289 background, *pyp1-1(H7L)*, the ripe fruit color turned orange (CCS55 line, Fig. 3e). The changes
290 in carotenoid profiles behind the fruit color shift were further investigated through HPLC-
291 UV/Vis analysis (Fig. 3b–d, f–h). The red fruit from the control lines, WT, WTEV21, *pyp1-*
292 *1(H7L)*, and 1-1EV11 contained predominantly lycopene and tiny amounts of other carotenoids,
293 including *β*-carotene, (*all E*) violaxanthin, and lutein (Fig. 3b–d, f–h). In addition, xanthophyll
294 esters were detected at a low level in the WT and hardly in the *pyp1-1(H7L)* background (Fig.
295 3d, h). In the ripe fruit of *CCS*-overexpression lines, regardless of WT or *pyp1-1(H7L)*
296 background, capsanthin was identified (Fig. 3b, f). The primary carotenoid of tomato, lycopene,
297 decreased while *β*-carotene, (*all E*) violaxanthin, and xanthophyll esters increased compared to
298 control lines (Fig. 3b–d, f–h).

299 **Alteration of carotenoid pathway and *β*-carotene enhancement in *CCS*-transformed tomato**

300 Carotenoid profiles in different tomato lines indicated the alteration of carotenoid
301 compositions (Figs.3&4a). Specifically, when total carotenoids in tomato fruit were quantified,

302 the fruit of WTCCS lines were all enhanced compared to WT and WTEV21 lines (Fig. 4b). Their
303 fruit had increments of 33–69% more compared to WT and WTEV21 lines. Nevertheless, total
304 carotenoids in 1-1CCS lines decreased by 20–28% compared to *pyp1-1(H7L)* and 1-1EV11 (Fig.
305 4b). In addition to total carotenoids, the carotenoid compositions were changed in *CCS*-
306 overexpression lines (Fig. 4c–g). In the red tomato of WT and *pyp1-1(H7L)* backgrounds, the
307 carotenoid fraction was mainly lycopene, which is the final carotenoid synthesized before the
308 pathway was split into *α*- or *β*-branches (Fig. 4c). Specifically, the amounts of lycopene, in WT
309 and WTEV21 lines, decreased from 85% of total carotenoids to 3–9% in WTCCS lines (Fig. 4c).
310 Similarly, in the mutant background, lycopene levels decreased from 87% of total carotenoids to
311 6–11% in *pyp1-1(H7L)* and 1-1EV11 (Fig. 4c).
312 Accordingly, other compositions downstream of the carotenoid pathway were altered
313 when *CCS* was overexpressed in both genetic backgrounds (Fig. 4d–g). Although the amounts of
314 carotenoid in the *α*-branch were much lower than total carotenoids, lycopene, and *β*-carotene, a
315 significant decrease of carotenoid contents in the *α*-branch was observed (Fig. 4d). In *α*-branch,
316 the amounts of *α*-carotene increased by 0.9–1.1-fold than the WT and WTEV21 lines, and 0.2–
317 0.5-fold than the *pyp1-1(H7L)* and 1-1EV11 lines (Fig. 4d). However, the lutein content
318 decreased by ~95% in both genetic backgrounds (Fig. 4d). Opposite to the decrease in total
319 amounts in the *α*-branch, most compositions, especially *β*-carotene, in *β*-branch were increased
320 in *CCS*-transformed fruit (Fig. 4e, f). Particularly, fruit *β*-carotene levels enhanced from 7 to 96–
321 105 μg g^{-1} f.wt. in WTCCS lines (Fig. 4e). Similarly, it increased from 6 to 41–45 μg g^{-1} f.wt. in
322 1-1CCS lines (Fig. 4e). Compared to WT and WTEV21 lines, about 11–14-fold increases were
323 observed in WTCCS lines (Fig. 4e). Although the increment was lower than the WT background,
324 still about 7–8-fold increases in *β*-carotene levels were observed in 1-1CCS lines compared to
325 *pyp1-1(H7L)* and 1-1EV11 lines (Fig. 4e). The other carotenoids in the *β*-branch also showed
326 significant changes in *CCS*-overexpression lines, although they took minor proportions in this
327 branch (Fig. 4e). Specifically, the amounts of zeaxanthin, antheraxanthin, and (*all E*)
328 violaxanthin were increased by 1.8–3.9, 3.6–4.5, and 2.5–3.2-fold in WTCCS lines than the WT
329 and WTEV21 lines (Fig. 4f). Similar increase patterns as WTCCS lines were observed in 1-
330 1CCS lines. Interestingly, the increase rate of zeaxanthin in 1-1CCS lines was 3.7–4.8-fold,
331 higher than in WTCCS lines (Fig. 4e). Since CCS is not native to tomato, no capsanthin or
332 capsorubin was detected in fruit from non-engineered or empty vector-transformed lines (Fig.

333 4e). However, the fruit of WTCCS lines contained capsanthin at levels of 0.74–1.14 μg g^{-1} f.wt.,
334 which was similar to the amounts in 1-1CCS lines. Capsorubin contents in the fruit of WTCCS
335 lines were 0.07 to 0.1μg g^{-1} f.wt., higher than 0.04–0.06 μg g^{-1} f.wt. accumulating in 1-1CCS
336 lines (Fig. 4e).
337 Free xanthophylls generated in both *a*- and *β*-branches can be esterified. Ripe fruit of WT
338 and WTEV21 lines accumulated 0.55–0.58 μg g^{-1} f.wt. xanthophyll esters (Fig. 3d, 3g). In
339 WTCCS lines, ripe fruit contained more xanthophyll esters at levels of 8–10 μg g^{-1} f.wt.,
340 increasing by 12.5–16.8-fold compared to the WT and WTEV21 lines (Fig. 3d, 3g). Although,
341 the *pyp1-1(H7L)* mutant was reported to produce no xanthophyll esters in flowers (Ariizumi *et*
342 *al.*, 2014), relatively small amounts of esters were detected in fruit at the level of ~0.1 μg g^{-1}
343 f.wt. (Fig. 3h & 3g). Moreover, the degree of xanthophyll esterification was elevated 3~6 times
344 when *CCS* was overexpressed in the mutant background (Fig. 3h, 3f).
345 The Pearson correlation analysis showed that the carotenoid pools in WTCCS and 1-
346 1CCS lines were altered in a similar fashion (Fig. 5). Capsanthin and capsorubin contents were
347 positively correlated with the accumulation of *a*-carotene, *β*-carotene, antheraxanthin, (*all E*)
348 violaxanthin, and xanthophyll esters when CCS was overexpressed in both backgrounds.
349 However, the alteration in total carotenoids by overexpressing *CCS* in the WT background
350 exhibited positive correlations with the amounts of capsanthin, capsorubin, and *β*-carotene,
351 opposite to 1-1CCS lines (Fig. 5).
352 **Phenotypic, carotenoid, and apocarotenoid compositional changes in tomato fruit of *CCS*-**
353 **derived hybrids**
354 To examine CCS function in the fruit of some large-fruited tomato of different genetic
355 backgrounds (Fig. 6a), varieties were selected to do controlled crosses with the transgenic line
356 from WTCCS46 or WTCCS59 lines '*CCS*-derived hybrids' or with WT 'Micro-Tom' to generate
357 'control-derived hybrids. Ripe fruit color from the selected maternal lines was red for 'FL7907B'
358 and 'LA2377', orange for 'Juane Flamme' and 'LA2374', and yellow for 'LA4044' (Fig. 6a).
359 The paternal lines WT 'Micro-Tom' and WTCCS (line 46) had red and orange ripe fruit color,
360 and different carotenoid compositions, respectively (Fig. 6a).
361 After crossing with WT 'Micro-Tom', the fruit of F1 hybrid with 'Juane Flamme',
362 'LA2374', and 'LA4044' turned red to different degrees while F1 hybrids with 'FL7907B' and
363 'LA2377' backgrounds remained unchanged (Fig. 6a). Tomato fruit from F1 hybrids of red

364 tomato varieties, ‘FL7907B’ x ‘Micro-Tom’ and ‘LA2377’ x ‘Micro-Tom’, the total carotenoids
365 in the fruit of control-derived lines were decreased by 11–18%, compared to their corresponding
366 maternal lines (Fig. 6b). When using orange and yellow tomato varieties as maternal parents,
367 fruit from F1 hybrids of ‘Juane Flamme’ x ‘Micro-Tom’ and ‘LA4044’ x ‘Micro-Tom’ showed
368 0.4 and 7.9-fold increase than their corresponding maternal lines respectively (Fig. 6b). No
369 difference was observed between fruits of ‘LA2374’ and ‘LA2374’ x ‘Micro-Tom’ (Fig. 6b).
370 Specifically, the lycopene contents of control-derived hybrids were increased by 2, 7.5 and 28-
371 fold for ‘Juane Flamme’ x ‘Micro-Tom’, ‘LA2374’ x ‘Micro-Tom’, and ‘LA4044’ x ‘Micro-
372 Tom’, but decreased by 0.11 and 0.19-fold for ‘FL7907B’ x ‘Micro-Tom’ and ‘LA2377’ x
373 ‘Micro-Tom’ respectively, compared to their corresponding maternal lines (Fig. 6b). Besides,
374 except for ‘LA4044’, the *β*-carotene amounts of control-derived hybrids were all decreased by 3–
375 57%, compared to their corresponding maternal lines (Fig. 6b).
376 When *CCS* was introduced into the genome of those tomato varieties, all fruit of *CCS*-
377 derived hybrids from these crosses showed color changing to orange, although their color
378 intensity varied depending on their maternal parents (Fig. 6a). Furthermore, the carotenoid
379 compositions were changed thoroughly compared to control-derived hybrids (Fig. 6b). The total
380 carotenoids of the fruits from *CCS*-derived hybrids were increased by 0.8–1.3-fold, compared to
381 their corresponding control-derived hybrids (Fig. 6a). Specifically, lycopene amounts were
382 significantly reduced by 63–92%, compared to their corresponding control-derived hybrids (Fig.
383 6b). The fold changes of *β*-carotene contents in the fruit from *CCS*-derived hybrids varied
384 depending on their maternal lines (Fig. 6b). Similar to Micro-Tom transformed with *CCS*, *β*-
385 carotene contents in the F1 hybrid tomato fruit generated from red tomato maternal varieties,
386 ‘FL7907B’ x ‘WTCCS’ and ‘LA2377’ x ‘WTCCS’, were increased from 2.1 and 6.7 to 185 and
387 145 μg g^{-1} f.wt. respectively, (Fig. 6b). In tomato fruit from F1 hybrids generated from orange
388 tomato maternal varieties, ‘Flamme’ x ‘WTCCS’ and ‘LA2374’ x ‘WTCCS’, *β*-carotene contents
389 were 226 and 122 μg g^{-1} f.wt., 2.6 and 1.5-fold more than their corresponding control-derived
390 hybrids (Fig. 6b). F1 hybrid fruit, ‘LA4044’ x ‘WTCCS’, accumulated 5.9 μg g^{-1} f.wt. *β*-
391 carotene, 35 times as in its control-derived hybrid (Fig. 6b). Except for ‘LA4044’, four other
392 CCS-derived hybrids showed 0.2–1.4-fold more *β*-carotene accumulating in fruits than their
393 paternal line, WTCCS46 (Fig. 6b).

394 In addition to changes in carotenes, capsanthin was detected at levels of 0.22–0.35 μg g^{-1}
395 f.wt. in the fruit of all CCS-derived hybrids, which were lower than the level of 0.74 μg g^{-1} f.wt.
396 in the fruit of the paternal line, WTCCS46 (Fig. 7a). Fruit of 'Flamme' x 'WTCCS' contained the
397 highest capsanthin content among all five F1 hybrids (Fig. 7a). In all fruit from of F1 *CCS*-
398 derived hybrids, the amounts of xanthophyll esters were significantly increased by 0.13–2.5-fold
399 and 1.3–2.7-fold compared to their corresponding maternal and control-derived hybrids
400 respectively (Fig. 7b). Fruit from 'Flamme' x 'WTCCS' contained the highest xanthophyll ester
401 content among all five F1 hybrids (Fig. 7b).
402 To test whether the volatile apocarotenoids derived from carotenoids, especially those
403 from lycopene and *β*-carotene, changed in *CCS*-derived hybrids, ripe fruits from control and
404 CCS-derived hybrids were collected and analyzed. In control-derived hybrids, 'Flamme' x
405 'Micro-Tom' and 'LA2374' x 'Micro-Tom' with orange fruit as one of the original parents
406 showed higher amounts of *β*-ionone and *β*-cyclocitral, compared to the other control-derived
407 hybrids (Fig. 8a&b). When *CCS* was overexpressed, both *β*-ionone and *β*-cyclocitral amounts
408 were increased by 1.3 to 13.0-fold and 2.7 to 19.1-fold in all five *CCS*-derived hybrids (Fig.
409 8a&b). The amounts of geranial, geranyl acetone, 6-methyl-5-hepten-2-one, and 6-methyl-5-
410 hepten-2-ol showed a decreasing trend in *CCS*-derived hybrids with one exception for 'LA2377'
411 x 'WTCCS' and the decrease in geranyl acetone was statistically significant (Fig. 8c–d).
412 **Retinol activity equivalents in engineered fruit**
413 To quantify the nutritional improvement of tomato via *CCS*-overexpression, we evaluated
414 retinol activity equivalents (RAE) computed based on bioactivities of vitamin A and provitamin
415 A (*β*-carotene, *β*-cryptoxanthin, and *a*-carotene) of ripe fruit pericarp from control and *CCS*-
416 overexpression lines ('Micro-Tom' background), as well as from the derived hybrids. No
417 difference in RAE was observed between the fruit of WT and WTEV21 (Fig. 9). Nevertheless,
418 fruit from WTCCS lines contained 662–875 μg retinol activity equivalents per 100g f.wt.
419 serving, respectively (Fig. 9). The RAE amounts in fruit from *CCS*-overexpression lines
420 increased by 9.2–13.5 times compared to WT and WTEV21 lines (Fig. 9). However, the RAE
421 amounts enhanced from 48.5–55.0 to 347–384 μg per 100g f.wt. when *CCS* was overexpressed
422 in the *pyp1-1(H7L)* background (Fig. 9). Importantly, the RAE amounts from the fruit of most
423 *CCS*-derived F1 hybrids were observed to be significantly higher levels than transgenic 'Micro-
424 Tom' overexpressing CCS (WTCCS46, Fig. 9). Specifically, the fruit of *CCS*-derived F1 hybrids,

425 ‘FL7907B’ x ‘WTCCS’, ‘LA2377’ x ‘WTCCS’, ‘Juane Flamme’ x ‘WTCCS’, ‘LA2374’ x
426 ‘WTCCS’, and ‘LA4044’ x ‘WTCCS’, contained RAE at levels of 1540, 1209, 1885, 1014, and
427 689 µg per 100g f.wt. serving, respectively, compared to their corresponding control-derived
428 hybrids at levels of 17, 56, 272, 172, and 49 µg per 100 g f.wt. (Fig. 9).
429

430 **Discussion**

431 Silencing of *CCS* in ripe pepper fruit was conducted to test its role in the carotenoid
432 pathway, which has not been investigated until this study (Fig. 1). The capsanthin and capsorubin
433 formation in fruit was abolished when CCS overexpression was knocked down, with a
434 concomitant change in pericarp color to yellow (Fig. 1a), resembling naturally occurring orange
435 and yellow peppers (Ha *et al.*, 2007; Guzman *et al.*, 2010). In pepper fruit, CCS draws the
436 carotenoid pathway to form a new sub-branch to produce ketocarotenoids, capsanthin and
437 capsorubin (Fig. 1e, f). When this sub-*β*-branch was abolished by VIGS, the flux went
438 downstream of main *β*-branch to accumulate abundant amounts of violaxanthin instead (Fig. 1b,
439 e). However, the flux was not retained in the main *β*-branch when *CCS* was silenced. In addition
440 to its function in capsanthin and capsorubin biosynthesis, CCS was reported to have LCYB
441 activity *in vitro* (Bouvier *et al.*, 1997; Mialoundama *et al.*, 2010). Consistent with this, silencing
442 of *CCS* reduced, both cyclization of lycopene and formation of ketocarotenoids. Thus, the
443 limited flow into the *β*-branch caused by the VIGS redirected the flux toward the *a*-branch, to
444 synthesize *a*-carotene and lutein (Fig. 1d).

445 We observed that the amounts of total carotenoids were reduced remarkably in *ccs*-
446 silenced fruit, suggesting that *CCS* also assisted in the accumulation of total carotenoids, with
447 more ketocarotenoids produced when CCS functioned normally (Fig. 1c, e). Both
448 ketocarotenoids might be preferable substrates for esterification than lutein and violaxanthin in
449 pepper (Fig. 1c, d, f). This was supported by our results that the reduction of capsanthin,
450 capsorubin, and their derivatives was paralleled by an increase of lutein and violaxanthin in *ccs*-
451 silenced fruit, while the esterification of lutein and violaxanthin did not complement the amounts
452 of xanthophyll esters (Fig. 3c), reported storage forms of the carotenoid pool (Li *et al.*, 2023).
453 Thus, lack of xanthophyll esterification might cause a flux reduction of the whole carotenoid
454 pathway. Overall, our results elucidated for the first time the critical role of CCS in the metabolic
455 flux and pool of the carotenoid pathway in pepper fruit, although the silencing effect of *CCS*
456 gene through VIGS has been tested in pepper previously (Fig. 1, Tian et al., 2015).

457 Previous research indicated that pepper LCYB had lycopene cyclization activity and
458 pepper CCS had catalyzed both capsanthin synthesis and lycopene cyclization *in vitro* (Bouvier
459 *et al.*, 1997; Mialoundama *et al.*, 2010), though these two proteins were not compared *in vivo*.
460 Using an *E. coli* expression platform engineered to produce up to lycopene in the carotenoid

461 synthetic pathway (Fig. 2a) or a strain that could produce xanthophylls (Fig. 2e), we compared
462 pepper CCS with the two tomato LYCBs. Under the same conditions, the *E. coli* strain harboring
463 pepper CCS showed a significantly higher ability to convert lycopene into *β*-carotene compared
464 to the strain containing either LCYB1 or LCYB2 (Fig. 2b–d). Our results are consistent with
465 CCS having a lower K_m to lycopene substrate compared to pepper LCYB in a previous study
466 (Mialoundama *et al.*, 2010). Accordingly, lycopene in the CCS-harbored strain was depleted by
467 CCS, and much more *β*-carotene was synthesized (Fig. 2d). In another scenario of capsanthin
468 biosynthesis (Fig. 2e), the *E. coli* strain containing CCS with pAC-VIOL plasmid produced
469 capsanthin successfully, while the expression of either LCYB1 or LCYB2 did not result in
470 capsanthin accumulation (Fig. 2f-h). These results proved that tomato LCYBs could not
471 synthesize ketocarotenoid, but CCS did function in capsanthin production in *E. coli*. Particularly,
472 pepper CCS and tomato LCYBs could increase the carotenoid flux downstream to produce more
473 carotenoids, including *β*-carotenes and xanthophylls, indicating that lycopene cyclization might
474 be a limited step in the carotenoid biosynthetic pathway, agreeing with previous studies (Moreno
475 *et al.*, 2020; Kössler *et al.*, 2021). These results suggested that CCS is superior for *in vivo*
476 modification of carotenoid pools by taking advantage of its multifunctional activities.
477 Given that CCS could change the flux in the carotenoid pathway based on its multiple
478 functions in pepper fruit and in engineered *E. coli*, and has not been used for directed
479 modification of carotenoid profiles of a ripening fruit yet, its overexpression in the fleshy fruit of
480 tomato allowed us to understand the sink strength in the carotenoid pathway, meanwhile
481 demonstrating the potential applications in crop biofortification. Here, we chose a tomato variety,
482 'Micro-Tom', including the WT and a mutant, *pyp1-1(H7L)*, to overexpress pepper *CCS*. Our
483 study showed that *CCS* overexpression did not significantly affect plant growth, development, or
484 yield (Fig. S3).
485 In tomato fruit, lycopene is the predominant carotenoid because the expression levels of
486 *LCYB* are relatively limited, constraining lycopene conversion to *β*-carotene (Pecker *et al.*, 1996;
487 Ronen *et al.*, 2000; Pandurangaiah *et al.*, 2016). CCS has been suggested to have evolved from
488 LCYB based on analyses of amino acid sequences (Fig. S4, (Mialoundama *et al.*, 2010), sharing
489 the same conserved motif, FLEET, and lycopene cyclase domain with LCYB (Fig. S5).
490 Supporting this, CCS proteins were phylogenetically related to moss LCYB-like 1 and 2 proteins
491 and other angiosperm LCYBs in the rooted phylogenetic tree (Fig. S4). The bottleneck of

492 lycopene cyclization in tomato fruit was alleviated by CCS, attributing to cyclization of more
493 lycopene into *β*-carotene (Fig. 4c, e). Here, the remarkable enhancement of *β*-carotene in tomato
494 fruit is comparable or superior to previous studies overexpressing *LCYB* gene in tomato (Rosati
495 *et al.*, 2000; D'Ambrosio *et al.*, 2004; Giorio *et al.*, 2008; Apel & Bock, 2009; Zhu *et al.*, 2020;
496 Mi *et al.*, 2022). Different from previous studies using LCYB, CCS also functioned in the
497 conversion of antheraxanthin and violaxanthin into capsanthin and capsorubin, respectively,
498 directing the carotenoid flux moving downstream further (Fig. 4). Besides, unlike previous
499 studies showing transgenic plants engineered with *LCYB* exhibiting tolerance to abiotic stresses
500 including salinity (Moreno *et al.*, 2021; Mi *et al.*, 2022), we observed no differences between
501 *CCS*-overexpression lines and control lines under salinity stress condition (Fig. S6).
502 Xanthophyll esters in red tomato of WT and WTEV lines represented only a small
503 proportion of carotenoids (Fig. 4g, D'Ambrosio et al., 2011). It differed from pepper since
504 limited free xanthophylls were accumulated in tomato fruit (Fig. 1c, Fig. 4c–f). However, the
505 increased flux in the carotenoid pathway by CCS allowed more xanthophylls to be synthesized
506 downstream than WT and WTEV lines (Fig. 4d–f), which were available for further esterification
507 (Fig. 4g). As a result, the proportion of xanthophyll esters in total carotenoids rose significantly
508 from 0.74–0.81% in WT and WTEV lines to 6.55–9.89% in WTCCS lines (Fig. 4f). Collectively,
509 total carotenoid, *β*-carotene, and xanthophylls (including zeaxanthin, antheraxanthin, (*all E*)
510 violaxanthin, capsanthin, and capsorubin) in the *β*-branch of WTCCS fruit increased along with
511 xanthophyll esters with positive correlation of 0.83, 0.92 and 0.87–0.96, respectively (Fig. 4, Fig.
512 5a), indicating the positive impact of xanthophyll esterification on carotenoid pools.
513 The xanthophyll esters in the mutant *pyp1-1(H7L)* were not completely missing as
514 expected, differing from a previous study (Ariizumi *et al.*, 2014). The total carotenoids and each
515 composition, except for xanthophyll esters, were similar among WT, WTEV21, *pyp1-1(H7L)*,
516 and 1-1EV11 lines (Fig. 3a–h, Fig. 4). However, the amounts of xanthophyll esters were at
517 relatively low levels, accounting for 0.14–0.16% of total carotenoids in *pyp1-1(H7L)* and 1-
518 1EV11 lines (Fig. 3h, Fig. 4g), much lower than WT and WTE21 lines. This result confirmed for
519 the first time that the mutant *pyp1-1(H7L)* had a limited ability to esterify xanthophylls.
520 Furthermore, it indicated that tiny amounts of xanthophyll esters, did not have an obvious impact
521 on the carotenoid pathway among WT, WTEV21, *pyp1-1(H7L)*, and 1-1EV11 lines (Fig. 3a–h,
522 Fig. 4). However, when *CCS* was overexpressed in *pyp1-1(H7L)*, the xanthophyll esters were

523 detectable but remained at relatively low levels of 0.86–1.36% of total carotenoids (Fig. 4g).
524 Although the gene encoding XAT1 is mutated in *pyp1-1(H7L)* (Ariizumi *et al.*, 2014), its paralog
525 XAT2 (Solyc02g094430) likely remains active in this mutant. *XAT2* expression level in all
526 tomato tissues is relatively low but slightly higher in fruit than in other tissues (CoNekT
527 database, Proost & Mutwil, 2018), thus contributing to this limited xanthophyll esterification.
528 Importantly, total carotenoids of 1-1CCS lines were significantly lower than *pyp1-1(H7L)* and 1-
529 1EV1, suggesting that in the absence of or low levels of xanthophyll esterification, the
530 production of total carotenoids and the flux to the *β*-branch are limited (Fig. 4). Besides, it was
531 reinforced by the correlation analysis that total carotenoids in 1-1CCS lines were negatively
532 associated with *β*-carotene, most free xanthophylls in *β*-branch and xanthophyll esters, contrary
533 to the alteration observed in WTCCS lines (Fig. 5).
534 We sought to answer why the fruit accumulated different xanthophyll esters between WT
535 and *pyp1-1(H7L)* when *CCS* was overexpressed. In a recent study, the accumulation of free
536 zeaxanthin was attributed to generating xanthophyll-derived apocarotenoids, which in turn
537 mediated feedback inhibition (D'Ambrosio *et al.*, 2023). This is supported by our observation
538 that zeaxanthin amounts in 1-1CCS fruit were significantly higher than in WTCCS lines but not
539 observed for other free xanthophylls of *β*-branch (Fig. 4f). The esterification in WTCCS lines
540 possibly kept xanthophylls in ester form, which were stably stored in plastoglobules and avoided
541 cleavage by CCDs (carotenoid cleavage dioxygenases) (DellaPenna and Pogson, 2006; Li et al.,
542 2023; D'Ambrosio et al., 2023).
543 Though 'Micro-Tom' is a convenient research model, it is dwarf with small fruit (Shikata
544 & Ezura, 2016). Hence, we selected five other large-fruited inbreds with different genetic
545 backgrounds to test *CCS* overexpression as a strategy to potentially improve their carotenoid
546 profiles. After crossing with 'Micro-Tom' WT or 'WTCCS', all derived F1 hybrids showed
547 similar plant growth and fruit size to their corresponding maternal lines, indicating that the
548 recessive dwarf allele from 'Micro-Tom' had no observable impact on growth and fruiting.
549 However, affected by introducing the genome of 'Micro-Tom WT' and 'WTCCS,' respectively,
550 the color of fruit from control- and *CCS*-derived hybrids was altered toward red and orange,
551 respectively, paralleling with the carotenoid compositional changes (Fig. 6). All *CCS*-derived
552 lines showed significantly higher total carotenoid levels in fruit compared to their corresponding
553 control-derived lines (Fig. 6b). Like the observation in WTCCS and 1-1CCS lines (Fig. 4b),

554 lycopene in the fruits of all five *CCS*-derived varieties was depleted and converted into *β*-
555 carotene under the catalysis of CCS (Fig. 6b). However, the accumulation of *β*-carotene in fruit
556 varied from one *CCS*-derived hybrid to another, among which four showed significantly higher
557 accumulation of *β*-carotene in fruit than its paternal line, 'WTCCS' (Fig. 6b).
558 In *CCS*-derived hybrids, 'FL7907B' x 'WTCCS' and 'LA2377' x 'WTCCS', the patterns
559 in carotenoid composition were similar to 'WTCCS' (Fig.3, Fig. 6b). *CCS* overexpression in
560 tomato possibly alleviated the limitation posed by the transcriptional regulation of genes in the
561 carotenoid-associated pathway (Duduit *et al.*, 2022), resulting in a higher metabolic flow moving
562 through lycopene cyclization. Their parental lines, 'FL7907B', 'LA2377' and 'Micro-Tom' WT,
563 had red fruit and accumulated dominantly lycopene but at different levels (Fig. 6b). The fruit of
564 'FL7907B' contained the highest amounts of lycopene among these three parental lines (Fig. 6b).
565 The greater the abundance of lycopene in parental lines, the greater were the amounts of *β*-
566 carotene in the fruit of *CCS*-derived hybrids (Fig. 6b). Consequently, 'FL7907B' x 'WTCCS'
567 accumulated the highest *β*-carotene contents among WTCCS lines, 'FL7907B' x 'WTCCS' and
568 'LA2377' x 'WTCCS' hybrids (Fig. 6b).
569 Previously, when *LCYB* gene was expressed in tomato varieties with red fruit, including
570 'Money Maker' (Rosati *et al.*, 2000; Dharmapuri *et al.*, 2002), 'Red Setter' (D'Ambrosio *et al.*,
571 2004), or 'Ailsa Craig' (Zhu *et al.*, 2020), higher accumulation of *β*-carotene in fruit was
572 observed. However, engineering carotenoid profiles in tomato with yellow or orange fruit is rare.
573 Two varieties, 'Juane Flamme' and 'LA2374', with orange fruit and higher *β*-carotene
574 accumulation when crossed to 'WTCCS' had even more improvement in *β*-carotene levels than
575 other parental lines.
576 The fruit of 'Juane Flamme' x 'WTCCS' contained the highest *β*-carotene among all
577 *CCS*-derived hybrids, which was near double that of 'LA2374' x 'WTCCS' (Fig. 6b). It was
578 possibly caused by the different promoter region sequence of *LCYB* (or *B* allele) between 'Juane
579 Flamme' and 'LA2374' reported previously, resulting in a higher *LCYB* expression in 'Juane
580 Flamme' (Orchard *et al.*, 2021). Hence, high expression of native *LCYB* in 'Juane Flamme' likely
581 coordinated with CCS to produce more *β*-carotene than other *CCS*-derived hybrids (Fig. 6b).
582 Another *CCS*-derived line, 'LA4044' x 'WTCCS', also showed a higher accumulation of *β*-
583 carotene although it was slightly lower than that found in the fruit of 'WTCCS' (Fig. 6b).
584 'LA4044' has yellow fruit flesh, in which deletion of 691 bp in the promoter region of *PSY* gene

585 resulted in its low expression level (Alseekh *et al.*, 2013; Shin *et al.*, 2019). It limited the flux to
586 carotenoids since PSY catalyzes the first committed step in the pathway. Consequently, the fruit
587 of 'LA4044' x 'WTCCS' accumulated considerably more *β*-carotene than its control-derived line
588 but lower than the other four *CCS*-derived hybrids (Fig. 6b).
589 Like 'Micro-Tom' WT transformed with CCS, the synthesis of capsanthin in *CCS*-derived
590 lines contributed to the increase in esterified xanthophylls (Fig. 7a). The high accumulation of
591 total carotenoids and *β*-carotene was positively associated with the accumulation of xanthophyll
592 esters (Fig. 4, Fig. 5). Reinforcing this, all five *CCS*-derived hybrids contained significantly
593 higher amounts of total carotenoids and *β*-carotene (Fig. 6b), and synergistically accumulated
594 more xanthophyll esters (Fig. 7b), compared to their corresponding control-derived hybrids. For
595 instance, the accumulation of xanthophyll esters in the fruit of 'LA4044' x 'WTCCS' was lower
596 than the other four *CCS*-derived lines, attributing to lower total carotenoids and *β*-carotene than
597 the other four *CCS*-derived hybrids (Fig. 6, Fig. 7).
598 Apocarotenoid volatiles are known to be generated in ripe fruit via oxidation of
599 carotenoid substates, among which *β*-ionone and *β*-cyclocitral are derived from *β*-carotene (Yoo
600 *et al.*, 2023). Apocarotenoid volatiles, including *β*-ionone, 6-methyl-5-hepten-2-one and
601 geranylacetone, have a positive impact on fruit flavor (Klee & Tieman, 2018; Kaur *et al.*, 2023)
602 and significant natural variation for them are found in wild relatives of tomato (Barnett *et al.*,
603 2023). Our results of volatile apocarotenoids suggested that higher accumulation of β-carotene in
604 the fruit of *CCS*-derived hybrids contributed to higher levels of *β*-ionone and *β*-cyclocitral (Fig.
605 8a&b). Accordingly, lycopene-derived apocarotenoids, geranial, 6-methyl-5-hepten-2-one, 6-
606 methyl-5-hepten-2-one and neral, showed decreased or increased or not changed depending upon
607 the genetic background of the line (Fig. 8c–f). These results are consistent with the hypothesis
608 that in ripe fruit of tomato plants *β*-carotene level is limiting for carotenoid cleavage dioxygenase
609 (CCD) involved in the synthesis of β-ionone and β-cyclocitral (Yoo *et al.*, 2023). The changes in
610 volatile apocarotenoids by overexpression of *CCS* with no yield drag could inspire new strategies
611 for improving tomato flavor, the trait most valued by the consumers (Tieman *et al.*, 2017).
612 Retinol activity equivalent (RAE) is used to evaluate the availability of vitamin A in food
613 (Institute of Medicine (US) Panel on Micronutrients, 2001). Unlike preformed vitamin A from
614 animal-based foods, provitamin A, mainly *β*-carotene from plant-based foods, is a healthier form
615 for long-term dietary intake since it requires further conversion after uptake and has not been

616 reported to have upper limitations (Blaner, 2020). In addition, the nutritional value is higher in
617 plant-based food in general based on nutrition density scores (Fig. S7). To evaluate the
618 nutritional significance of *CCS*-engineered tomato lines, including 'Micro-Tom' (WTCCS and 1-
619 1CCS lines) and *CCS*-derived hybrids, we summarized the RAE value from the fruit of these
620 engineered tomato lines along with those from representative vegetables and fruits (Fig. 9).
621 As a widely consumed vegetable, commercial tomatoes in red, orange, and yellow colors
622 contain limited provitamin A, much lower than many other vegetables and fruits (Fig. 9). *CCS*-
623 engineered tomato reported here is a significantly better food source than currently available
624 tomatoes, comparable to other high RAE vegetables and fruits or even better (Fig. 9). In
625 particular, the RAE amounts in ripe fruit of WTCCS were comparable to carrots (Fig. 9).
626 However, in 1-1CCS lines, the increases in RAE were constrained possibly because of the
627 limited ability in xanthophyll esterification, so that the RAE values were lower than WTCCS
628 lines (Fig. 9). Surprisingly, the fruit from *CCS*-derived hybrid showed even higher RAE values
629 contributed from high *β*-carotene accumulation (Fig. 6b), among which four of them were higher
630 than male RDA in a serving (Fig. 9), indicating the successful biofortification in different
631 commercially viable tomato varieties. In addition to fruits and vegetables, the fruit of *CCS*-
632 engineered tomato lines, including WTCCS, 1-1CCS, and *CCS*-derived hybrids, were
633 comparable or even superior to other engineered crop plants in RAE value (Giuliano, 2017). For
634 instance, compared to the first tomato ('MoneyMaker') engineered with *LCYB* gene from
635 *Arabidopsis* containing ~458 µg RAE per 100 g serving (Rosati et al., 2000), here, RAE values
636 from the fruit of WTCCS lines and *CCS*-derived hybrids were significantly improved (Fig. 9).
637 Golden rice contains up to 258 µg RAE per 100 g serving (Paine *et al.*, 2005), which requires
638 271 and 349 g serving to meet female and male RDA, respectively. In this study, the
639 consumption of 80–106 and 103–136 g of WTCCS fruit, 182–202 and 235–260 g of 1-1CCS
640 fruit, 37–102 and 48–131 g of *CCS*-derived hybrid fruit meets female and male RDA,
641 respectively (Fig. 9). A demographic survey documented the lack of good vitamin A
642 consumption in 12 East African countries (Wolde & Tessema, 2023). *CCS*-engineered tomato
643 with high provitamin A is a healthy and safe food source for combating VAD in developing
644 nations. Besides, *CCS* overexpression in different tomato varieties could provide adequate
645 options for catering to consumers' demands.

646 In addition to provitamin A, capsanthin and capsorubin are reported to be potentially
647 beneficial for human health (Maoka *et al.*, 2001; Molnár *et al.*, 2005, 2012; Fernández-García *et*
648 *al.*, 2016; Jo *et al.*, 2017; Joo *et al.*, 2021; Kennedy *et al.*, 2021; Shanmugham & Subban, 2022).
649 This study is the first report on accumulation of capsanthin and capsorubin in a fleshy fruit
650 through metabolic engineering. Previously, ketocarotenoids were reported to accumulate in
651 flower (*Viola cornuta* L.) and rice endosperm (Ha *et al.*, 2019; Jeong *et al.*, 2021). Pepper *CCS*,
652 combined with different expression cassettes harboring carotenogenesis gene(s), was introduced
653 into rice to generate grain accumulating up to 0.4 μg/g capsanthin and capsorubin in the
654 endosperm (Ha *et al.*, 2019). By only overexpressing the pepper *CCS* we reached comparable
655 results. Ketocarotenoids in WTCCS and 1-1CCS fruit accumulated at higher levels (Fig. 4f) than
656 in rice grain reported previously, while they were at similar levels in the fruits of all five F1
657 *CCS*-derived hybrids (Fig. 7a). Capsanthin has been reported to protect mice against hepatic
658 steatosis and steatohepatitis in nonalcoholic fatty liver disease (Joo *et al.*, 2021). A high fat diet
659 with 0.5 μg g^{-1} capsanthin, similar to the contents in CCS-engineered fruit, generated a
660 protective effect. (Joo *et al.*, 2021).
661 In summary, constitutive expression of pepper *CCS* in 'Micro-Tom', *pyp1-1(H7L)*
662 mutant, and selected tomato varieties with different genetic backgrounds altered the metabolic
663 flux in the carotenoid pathway (Fig. 10). The carotenoid flux moved toward *β*-branch under the
664 function of CCS, producing remarkably higher provitamin A, *β*-carotene (Fig. 10). Furthermore,
665 considerable amounts of capsanthin and capsorubin accumulated in *CCS*-engineered tomato (Fig.
666 10). Along with the production of specialized ketocarotenoids, other xanthophylls of the *β*-
667 branch were accumulated more in *CCS*-engineered tomato fruit, contributing to xanthophyll
668 esterification (Fig. 10). Our results on the mutant, *pyp1-1(H7L)*, revealed that xanthophyll esters
669 had key regulatory impacts on the carotenoid accumulation in tomato fruit, facilitating the whole
670 carotenoid flux (Fig. 10). This study demonstrated that CCS could function under different
671 genetic backgrounds, contributing to the accumulation of total carotenoids, *β*-carotene,
672 ketocarotenoids and *β*-carotene-derived apocarotenoids in tomato fruit, consequently enhancing
673 its color, flavor and nutritional value.

674 **Acknowledgments**
675 We gratefully acknowledge the funding support from the Horticultural Sciences Department,
676 University of Florida as a graduate assistantship to J.F. B.R.'s research was supported by a grant
677 from Florida Department of Agriculture and Consumer services via the USDA Specialty Crops
678 Block Grant program. We gratefully acknowledge the kind donation of an *E. coli* strain, SixPack
679 by Dr. Gyorgy Posfai and Dr. Zsuzsanna Gyorfy both from the Biological Research Centre of the
680 Hungarian Academy of Sciences.
681 **Competing Interest Statement:** The authors declare no competing interests.
682 **Author Contributions:** J.F. and B.R. planned the study, J.F. conducted the experimental work
683 on pepper VIGS, carotenoid production in *E. coli* and transgenic tomato, D.T. conducted the
684 work on fruit volatiles and J.F wrote the first draft, and all authors contributed to writing and
685 editing the final draft.
686 **Data availability statement:** All pertinent data are included in the submission.

687 References

688 **Alseekh S, Ofner I, Pleban T, Tripodi P, Di Dato F, Cammareri M, Mohammad A,**
689 **Grandillo S, Fernie AR, Zamir D**. **2013**. Resolution by recombination: Breaking up Solanum
690 pennellii introgressions. *Trends in Plant Science* **18**: 536–538.
691 **Apel W, Bock R**. **2009**. Enhancement of carotenoid biosynthesis in transplastomic tomatoes by
692 induced lycopene-to-provitamin a conversion. *Plant Physiology* **151**: 59–66.
693 **Ariizumi T, Kishimoto S, Kakami R, Maoka T, Hirakawa H, Suzuki Y, Ozeki Y, Shirasawa**
694 **K, Bernillon S, Okabe Y, *et al.* 2014**. Identification of the carotenoid modifying gene PALE
695 YELLOW PETAL 1 as an essential factor in xanthophyll esterification and yellow flower
696 pigmentation in tomato (Solanum lycopersicum). *Plant Journal* **79**: 453–465.
697 **Barnett JR, Tieman DM, Caicedo AL**. **2023**. Variation in ripe fruit volatiles across the tomato
698 clade: An evolutionary framework for studying fruit scent diversity in a crop wild relative.
699 *American Journal of Botany* **110**: 1–14.
700 **Berry HM, Rickett D V., Baxter CJ, Enfissi EMA, Fraser PD**. **2019**. Carotenoid biosynthesis
701 and sequestration in red chilli pepper fruit and its impact on colour intensity traits. *Journal of*
702 *Experimental Botany* **70**: 2637–2650.
703 **Blaner WS**. **2020**. Chapter 5 - Vitamin A and provitamin A carotenoids. In: Marriott BP, Birt DF,
704 Stallings VA, Yates AA, eds. Present Knowledge in Nutrition (Eleventh Edition). Academic
705 Press, 73–91.
706 **Bouvier F, D'Harlingue A, Camara B**. **1997**. Molecular analysis of carotenoid cyclase
707 inhibition. *Archives of Biochemistry and Biophysics* **346**: 53–64.
708 **Bouvier F, Hugueney P, D'Harlingue A, Kuntz M, Camara B**. **1994**. Xanthophyll
709 biosynthesis in chromoplasts: isolation and molecular cloning of an enzyme catalyzing the
710 conversion of 5,6-epoxycarotenoid into ketocarotenoid. *The Plant Journal* **6**: 45–54.
711 **Butelli E, Titta L, Giorgio M, Mock HP, Matros A, Peterek S, Schijlen EGWM, Hall RD,**
712 **Bovy AG, Luo J, *et al.* 2008**. Enrichment of tomato fruit with health-promoting anthocyanins by
713 expression of select transcription factors. *Nature Biotechnology* **26**: 1301–1308.
714 **Cheng Y, Pang X, Wan H, Ahammed GJ, Yu J, Yao Z, Ruan M, Ye Q, Li Z, Wang R, *et al.***
715 **2017**. Identification of optimal reference genes for normalization of qPCR analysis during
716 pepper fruit development. *Frontiers in Plant Science* **8**: 1–14.

717 **Chetty VJ, Ceballos N, Garcia D, Narváez-Vásquez J, Lopez W, Orozco-Cárdenas ML**.
718 **2013**. Evaluation of four Agrobacterium tumefaciens strains for the genetic transformation of
719 tomato (Solanum lycopersicum L.) cultivar Micro-Tom. *Plant Cell Reports* **32**: 239–247.
720 **Classic Murashige T, Skoog F**. **1962**. A revised medium for rapid growth and bioassays with
721 tobacco tissue cultures. *Physiol. Plant* **15**: 473–497.
722 **Cunningham FX, Lee H, Gantt E**. **2007**. Carotenoid biosynthesis in the primitive red alga
723 Cyanidioschyzon merolae. *Eukaryotic Cell* **6**: 533–545.
724 **Cunningham FX, Sun Z, Chamovitz D, Hirschberg J, Gantt E**. **1994**. Molecular structure and
725 enzymatic function of lycopene cyclase from the cyanobacterium Synechococcus sp strain
726 PCC7942. *The Plant Cell* **6**: 1107–1121.
727 **Cvetković D, Marković D**. **2008**. UV-effects on antioxidant activity of selected carotenoids in
728 the presence of lecithin estimated by DPPH test. *Journal of the Serbian Chemical Society* **73**:
729 1051–1061.
730 **D'Ambrosio C, Giorio G, Marino I, Merendino A, Petrozza A, Salfi L, Stigliani AL, Cellini**
731 **F**. **2004**. Virtually complete conversion of lycopene into β-carotene in fruits of tomato plants
732 transformed with the tomato lycopene β-cyclase (tlcy-b) cDNA. *Plant Science* **166**: 207–214.
733 **D'Ambrosio C, Stigliani AL, Giorio G**. **2011**. Overexpression of CrtR-b2 (carotene beta
734 hydroxylase 2) from S. lycopersicum L. differentially affects xanthophyll synthesis and
735 accumulation in transgenic tomato plants. *Transgenic Research* **20**: 47–60.
736 **D'Ambrosio C, Stigliani AL, Rambla JL, Frusciante S, Diretto G, Enfissi EMA, Granell A,**
737 **Fraser PD, Giorio G**. **2023**. A xanthophyll-derived apocarotenoid regulates carotenogenesis in
738 tomato chromoplasts. *Plant Science* **328**: 111575.
739 **Delgado-Pelayo R, Hornero-Méndez D**. **2012**. Identification and quantitative analysis of
740 carotenoids and their esters from sarsaparilla (Smilax aspera L.) berries. *Journal of Agricultural*
741 *and Food Chemistry* **60**: 8225–8232.
742 **Dharmapuri S, Rosati C, Pallara P, Aquilani R, Bouvier F, Camara B, Giuliano G**. **2002**.
743 Metabolic engineering of xanthophyll content in tomato fruits. *FEBS Letters* **519**: 30–34.
744 **Duduit JR, Kosentka PZ, Miller MA, Blanco-Ulate B, Lenucci MS, Panthee DR, Perkins-**
745 **Veazie P, Liu W**. **2022**. Coordinated transcriptional regulation of the carotenoid biosynthesis
746 contributes to fruit lycopene content in high-lycopene tomato genotypes. *Horticulture Research*
747 **9**: 1–17.

748 **Fernández-García E, Carvajal-Lérida I, Pérez-Gálvez A**. **2016**. Carotenoids exclusively
749 synthesized in red pepper (capsanthin and capsorubin) protect human dermal fibroblasts against
750 UVB induced DNA damage. *Photochemical and Photobiological Sciences* **15**: 1204–1211.
751 **Fitzpatrick TB, Basset GJC, Borel P, Carrari F, DellaPenna D, Fraser PD, Hellmann H,**
752 **Osorio S, Rothan C, Valpuesta V, *et al.* 2012**. Vitamin deficiencies in humans: Can plant
753 science help? *Plant Cell* **24**: 395–414.
754 **Furubayashi M, Kubo A, Takemura M, Otani Y, Maoka T, Terada Y, Yaoi K, Ohdan K,**
755 **Misawa N, Mitani Y**. **2021**. Capsanthin Production in Escherichia coli by Overexpression of
756 Capsanthin/Capsorubin Synthase from Capsicum annuum. *Journal of Agricultural and Food*
757 *Chemistry* **69**: 5076–5085.
758 **Giorio G, Stigliani AL, D'Ambrosio C**. **2008**. Over-expression of carotene β-hydroxylase 1
759 (CrtR-b1) and lycopene β-cyclase (Lcy-b) in transgenic tomato fruits. *Acta Horticulturae* **789**:
760 277–284.
761 **Giuliano G**. **2017**. Provitamin A biofortification of crop plants: a gold rush with many miners.
762 *Current Opinion in Biotechnology* **44**: 169–180.
763 **Grune T, Lietz G, Palou A, Ross AC, Stahl W, Tang G, Thurnham D, Yin S, Biesalski HK**.
764 **2010**. β-Carotene Is an Important Vitamin A Source for Humans. *The Journal of Nutrition* **140**:
765 2268S-2285S.
766 **Guzman I, Hamby S, Romero J, Bosland PW, O'Connell MA**. **2010**. Variability of carotenoid
767 biosynthesis in orange colored Capsicum spp. *Plant Science* **179**: 49–59.
768 **Ha SH, Kim JK, Jeong YS, You MK, Lim SH, Kim JK**. **2019**. Stepwise pathway engineering
769 to the biosynthesis of zeaxanthin, astaxanthin and capsanthin in rice endosperm. *Metabolic*
770 *Engineering* **52**: 178–189.
771 **Ha SH, Kim JB, Park JS, Lee SW, Cho KJ**. **2007**. A comparison of the carotenoid
772 accumulation in Capsicum varieties that show different ripening colours: Deletion of the
773 capsanthin-capsorubin synthase gene is not a prerequisite for the formation of a yellow pepper.
774 *Journal of Experimental Botany* **58**: 3135–3144.
775 **Institute of Medicine (US) Panel on Micronutrients**. **2001**. *Dietary Reference Intakes for*
776 *Vitamin A, Vitamin K, Arsenic, Boron, Chromium, Copper, Iodine, Iron, Manganese,*
777 *Molybdenum, Nickel, Silicon, Vanadium, and Zinc*. Washington, D.C.: National Academies Press
778 (US).

Jeong YS, Kim JK, Baek SA, Lee JY, Lee D, Ha SH. **2021**. Reciprocal Crosses Between Astaxanthin and Capsanthin Rice Unravel Effects of Metabolic Gene Efficacy in Rice Endosperm. *Journal of Plant Biology* **64**: 371–377.

Jo SJ, Kim JW, Choi HO, Kim JH, Kim HJ, Woo SH, Han BH. **2017**. Capsanthin inhibits both adipogenesis in 3T3-L1 preadipocytes and weight gain in high-fat diet-induced obese mice. *Biomolecules and Therapeutics* **25**: 329–336.

Joo HK, Lee YR, Lee EO, Kim S, Jin H, Kim S, Lim YP, An CG, Jeon BH. **2021**. Protective Role of Dietary Capsanthin in a Mouse Model of Nonalcoholic Fatty Liver Disease. *Journal of Medicinal Food* **24**: 635–644.

Kanwar P, Ghosh S, Sanyal SK, Pandey GK. **2022**. Identification of Gene Copy Number in the Transgenic Plants by Quantitative Polymerase Chain Reaction (qPCR). In: Methods in Molecular Biology. Humana, New York, NY, 161–171.

Kaur G, Abugu M, Tieman D. **2023**. The dissection of tomato flavor: biochemistry, genetics, and omics. *Frontiers in Plant Science* **14**: 1–18.

Kennedy LE, Abraham A, Kulkarni G, Shettigar N, Dave T, Kulkarni M. **2021**. Capsanthin, a Plant-Derived Xanthophyll: a Review of Pharmacology and Delivery Strategies. *AAPS PharmSciTech* **22**.

Kim S, Ha TY, Hwang IK. **2009**. Analysis, bioavailability, and potential healthy effects of capsanthin, natural red pigment from capsicum spp. *Food Reviews International* **25**: 198–213.

Kim J, Park M, Jeong ES, Lee JM, Choi D. **2017**. Harnessing anthocyanin-rich fruit: A visible reporter for tracing virus-induced gene silencing in pepper fruit. *Plant Methods* **13**: 1–10.

Klee HJ, Tieman DM. **2018**. The genetics of fruit flavour preferences. *Nature Reviews Genetics* **19**: 347–356.

Kössler S, Armarego-Marriott T, Tarkowská D, Turečková V, Agrawal S, Mi J, De Souza LP, Schöttler MA, Schadach A, Fröhlich A, *et al.* 2021. Lycopene β-cyclase expression influences plant physiology, development, and metabolism in tobacco plants. *Journal of Experimental Botany* **72**: 2544–2569.

Kraemer K, Waelti M, De Pee S, Moench-Pfanner R, Hathcock JN, Bloem MW, Semba RD. **2008**. Are low tolerable upper intake levels for vitamin A undermining effective food fortification efforts? *Nutrition Reviews* **66**: 517–525.

809 **Lee PC, Schmidt-Dannert C**. **2002**. Metabolic engineering towards biotechnological production
810 of carotenoids in microorganisms. *Applied Microbiology and Biotechnology* **60**: 1–11.
811 **Li R, Zeng Q, Zhang X, Jing J, Ge X, Zhao L, Yi B, Tu J, Fu T, Wen J, *et al.* 2023**.
812 Xanthophyll esterases in association with fibrillins control the stable storage of carotenoids in
813 yellow flowers of rapeseed (Brassica juncea). *New Phytologist*.
814 **Lipinszki Z, Vernyik V, Farago N, Sari T, Puskas LG, Blattner FR, Posfai G, Gyorfy Z**.
815 **2018**. Enhancing the Translational Capacity of E. coli by Resolving the Codon Bias. *ACS*
816 *Synthetic Biology* **7**: 2656–2664.
817 **Liu Y, Schiff M, Dinesh-Kumar SP**. **2002**. Virus-induced gene silencing in tomato. *The Plant*
818 *Journal* **31**: 777–786.
819 **Maoka T, Fujiwara Y, Hashimoto K, Akimoto N**. **2001**. Capsanthone 3,6-epoxide, a new
820 carotenoid from the fruits of the red paprika Capsicum annuum L. *Journal of Agricultural and*
821 *Food Chemistry* **49**: 3965–3968.
822 **Maquilan MAD, Padilla DC, Dickson DW, Rathinasabapathi B**. **2020**. Improved resistance to
823 root-knot nematode species in an advanced inbred line of specialty pepper (Capsicum annuum).
824 *HortScience* **55**: 1105–1110.
825 **Mi J, Vallarino JG, Petřík I, Novák O, Correa SM, Chodasiewicz M, Havaux M,**
826 **Rodriguez-Concepcion M, Al-Babili S, Fernie AR, *et al.* 2022**. A manipulation of carotenoid
827 metabolism influence biomass partitioning and fitness in tomato. *Metabolic Engineering* **70**:
828 166–180.
829 **Mialoundama AS, Heintz D, Jadid N, Nkeng P, Rahier A, Deli J, Camara B, Bouvier F**.
830 **2010**. Characterization of plant carotenoid cyclases as members of the flavoprotein family
831 functioning with no net redox change. *Plant Physiology* **153**: 970–979.
832 **Mínguez-Mosquera MI, Hornero-Méndez D**. **1993**. Separation and Quantification of the
833 Carotenoid Pigments in Red Peppers (Capsicum annuum L.), Paprika, and Oleoresin by
834 Reversed-Phase HPLC. *Journal of Agricultural and Food Chemistry* **41**: 1616–1620.
835 **Molnár P, Kawase M, Satoh K, Sohara Y, Tanaka T, Tani S, Sakagami H, Nakashima H,**
836 **Motohashi N, Gyémánt N, *et al.* 2005**. Biological activity of carotenoids in red paprika,
837 Valencia orange and Golden delicious apple. *Phytotherapy Research* **19**: 700–707.
838 **Molnár J, Serly J, Pusztai R, Vincze I, Molnár P, Horváth G, Deli J, Maoka T, Zalatnai A,**
839 **Tokuda H, *et al.* 2012**. Putative supramolecular complexes formed by carotenoids and

840 xanthophylls with ascorbic acid to reverse multidrug resistance in cancer cells. *Anticancer*
841 *Research* **32**: 507–517.
842 **Moreno JC, Martinez-Jaime S, Kosmacz M, Sokolowska EM, Schulz P, Fischer A,**
843 **Luzarowska U, Havaux M, Skirycz A**. **2021**. A Multi-OMICs Approach Sheds Light on the
844 Higher Yield Phenotype and Enhanced Abiotic Stress Tolerance in Tobacco Lines Expressing the
845 Carrot lycopene β-cyclase1 Gene. *Frontiers in Plant Science* **12**: 1–17.
846 **Moreno JC, Mi J, Agrawal S, Kössler S, Turečková V, Tarkowská D, Thiele W, Al-Babili S,**
847 **Bock R, Schöttler MA**. **2020**. Expression of a carotenogenic gene allows faster biomass
848 production by redesigning plant architecture and improving photosynthetic efficiency in tobacco.
849 *The Plant Journal*: tpj.14909.
850 **Neuman H, Galpaz N, Cunningham FX, Zamir D, Hirschberg J**. **2014**. The tomato mutation
851 nxd1 reveals a gene necessary for neoxanthin biosynthesis and demonstrates that violaxanthin is
852 a sufficient precursor for abscisic acid biosynthesis. *Plant Journal* **78**: 80–93.
853 **Nishino A, Yasui H, Maoka T**. **2016**. Reaction of Paprika Carotenoids, Capsanthin and
854 Capsorubin, with Reactive Oxygen Species. *Journal of Agricultural and Food Chemistry* **64**:
855 4786–4792.
856 **Orchard CJ, Cooperstone JL, Gas-Pascual E, Andrade MC, Abud G, Schwartz SJ, Francis**
857 **DM**. **2021**. Identification and assessment of alleles in the promoter of the Cyc-B gene that
858 modulate levels of β-carotene in ripe tomato fruit. *Plant Genome* **14**.
859 **Paine JA, Shipton CA, Chaggar S, Howells RM, Kennedy MJ, Vernon G, Wright SY,**
860 **Hinchliffe E, Adams JL, Silverstone AL, *et al.* 2005**. Improving the nutritional value of Golden
861 Rice through increased pro-vitamin A content. *Nature Biotechnology* **23**: 482–487.
862 **Pandurangaiah S, Ravishankar K V., Shivashankar KS, Sadashiva AT, Pillakenchappa K,**
863 **Narayanan SK**. **2016**. Differential expression of carotenoid biosynthetic pathway genes in two
864 contrasting tomato genotypes for lycopene content. *Journal of Biosciences* **41**: 257–264.
865 **Pecker I, Gabbay R, Cunningham FX, Hirschberg J**. **1996**. Cloning and characterization of
866 the cDNA for lycopene beta-cyclase from tomato reveals decrease in its expression during fruit
867 ripening. *Plant Molecular Biology* **30**: 807–819.
868 **Proost S, Mutwil M**. **2018**. CoNekT: An open-source framework for comparative genomic and
869 transcriptomic network analyses. *Nucleic Acids Research* **46**: W133–W140.

870 **Ronen G, Carmel-Goren L, Zamir D, Hirschberg J**. **2000**. An alternative pathway to β-
871 carotene formation in plant chromoplasts discovered by map-based cloning of Beta and old-gold
872 color mutations in tomato. *Proceedings of the National Academy of Sciences of the United States*
873 *of America* **97**: 11102–11107.
874 **Rosati C, Aquilani R, Dharmapuri S, Pallara P, Marusic C, Tavazza R, Bouvier F, Camara**
875 **B, Giuliano G**. **2000**. Metabolic engineering of beta-carotene and lycopene content in tomato
876 fruit. *Plant Journal* **24**: 413–420.
877 **Saito T, Ariizumi T, Okabe Y, Asamizu E, Hiwasa-Tanase K, Fukuda N, Mizoguchi T,**
878 **Yamazaki Y, Aoki K, Ezura H**. **2011**. TOMATOMA: A novel tomato mutant database
879 distributing micro-tom mutant collections. *Plant and Cell Physiology* **52**: 283–296.
880 **Shanmugham V, Subban R**. **2022**. Capsanthin from Capsicum annum fruits exerts anti-
881 glaucoma, antioxidant, anti-inflammatory activity, and corneal pro-inflammatory cytokine gene
882 expression in a benzalkonium chloride-induced rat dry eye model. *Journal of Food Biochemistry*
883 **46**: 1–16.
884 **Shikata M, Ezura H**. **2016**. Micro-Tom Tomato as an Alternative Plant Model System: Mutant
885 Collection and Efficient Transformation. In: Methods in Molecular Biology. 47–55.
886 **Shin JH, Yoo HJ, Yeam I, Lee JM**. **2019**. Distinguishing two genetic factors that control yellow
887 fruit color in tomato. *Horticulture Environment and Biotechnology* **60**: 59–67.
888 **Van Der Straeten D, Bhullar NK, De Steur H, Gruissem W, MacKenzie D, Pfeiffer W, Qaim**
889 **M, Slamet-Loedin I, Strobbe S, Tohme J, *et al.* 2020**. Multiplying the efficiency and impact of
890 biofortification through metabolic engineering. *Nature Communications* **11**: 1–10.
891 **Sun HJ, Uchii S, Watanabe S, Ezura H**. **2006**. A highly efficient transformation protocol for
892 Micro-Tom, a model cultivar for tomato functional genomics. *Plant and Cell Physiology* **47**:
893 426–431.
894 **Tian SL, Li L, Shah SNM, Gong ZH**. **2015**. The relationship between red fruit colour
895 formation and key genes of capsanthin biosynthesis pathway in Capsicum annuum. *Biologia*
896 *Plantarum* **59**: 507–513.
897 **Tieman DM, Zeigler M, Schmelz EA, Taylor MG, Bliss P, Kirst M, Klee HJ**. **2006**.
898 Identification of loci affecting flavour volatile emissions in tomato fruits. *Journal of*
899 *Experimental Botany* **57**: 887–896.

900 **Tieman D, Zhu G, Resende MFR, Lin T, Nguyen C, Bies D, Rambla JL, Beltran KSO,**
901 **Taylor M, Zhang B, *et al.* 2017**. A chemical genetic roadmap to improved tomato flavor.
902 *Science (New York, N.Y.)* **355**: 391–394.
903 **Trajković M, Jevremovic S, Dragićević M, Simonović AD, Subotić AR, Miloševi S, Cingel**
904 **A**. **2021**. Alteration of flower color in viola Cornuta cv. "lutea splendens" through metabolic
905 engineering of Capsanthin/Capsorubin synthesis. *Horticulturae* **7**.
906 **Wahyuni Y, Ballester A-R, Sudarmonowati E, Bino RJ, Bovy AG**. **2011**. Metabolite
907 biodiversity in pepper (Capsicum) fruits of thirty-two diverse accessions: Variation in health-
908 related compounds and implications for breeding. *Phytochemistry* **72**: 1358–1370.
909 **Wahyuni Y, Ballester AR, Sudarmonowati E, Bino RJ, Bovy AG**. **2013**. Secondary
910 metabolites of Capsicum species and their importance in the human diet. *Journal of Natural*
911 *Products* **76**: 783–793.
912 **Wolde M, Tessema ZT**. **2023**. Determinants of good vitamin A consumption in the 12 East
913 Africa Countries using recent Demographic and health survey. *PLoS ONE* **18**: 1–15.
914 **Xu S, Gao S, An Y**. **2023**. Research progress of engineering microbial cell factories for pigment
915 production. *Biotechnology Advances* **65**: 108150.
916 **Ye X, Beyer P**. **2000**. Engineering the provitamin A (β-carotene) biosynthetic pathway into
917 (carotenoid-free) rice endosperm. *Science* **287**: 303–305.
918 **Yoo HJ, Chung MY, Lee HA, Lee S Bin, Grandillo S, Giovannoni JJ, Lee JM**. **2023**. Natural
919 overexpression of CAROTENOID CLEAVAGE DIOXYGENASE 4 in tomato alters carotenoid
920 flux. *Plant Physiology* **192**: 1289–1306.
921 **Zheng X, Giuliano G, Al-Babili S**. **2020**. Carotenoid biofortification in crop plants: citius,
922 altius, fortius. *Biochimica et Biophysica Acta - Molecular and Cell Biology of Lipids* **1865**.
923 **Zhu K, Zheng X, Ye J, Jiang Q, Chen H, Mei X, Wurtzel ET, Deng X**. **2020**. Building the
924 synthetic biology toolbox with enzyme variants to expand opportunities for biofortification of
925 provitamin a and other health-promoting carotenoids. *Journal of Agricultural and Food*
926 *Chemistry* **68**: 12048–12057.

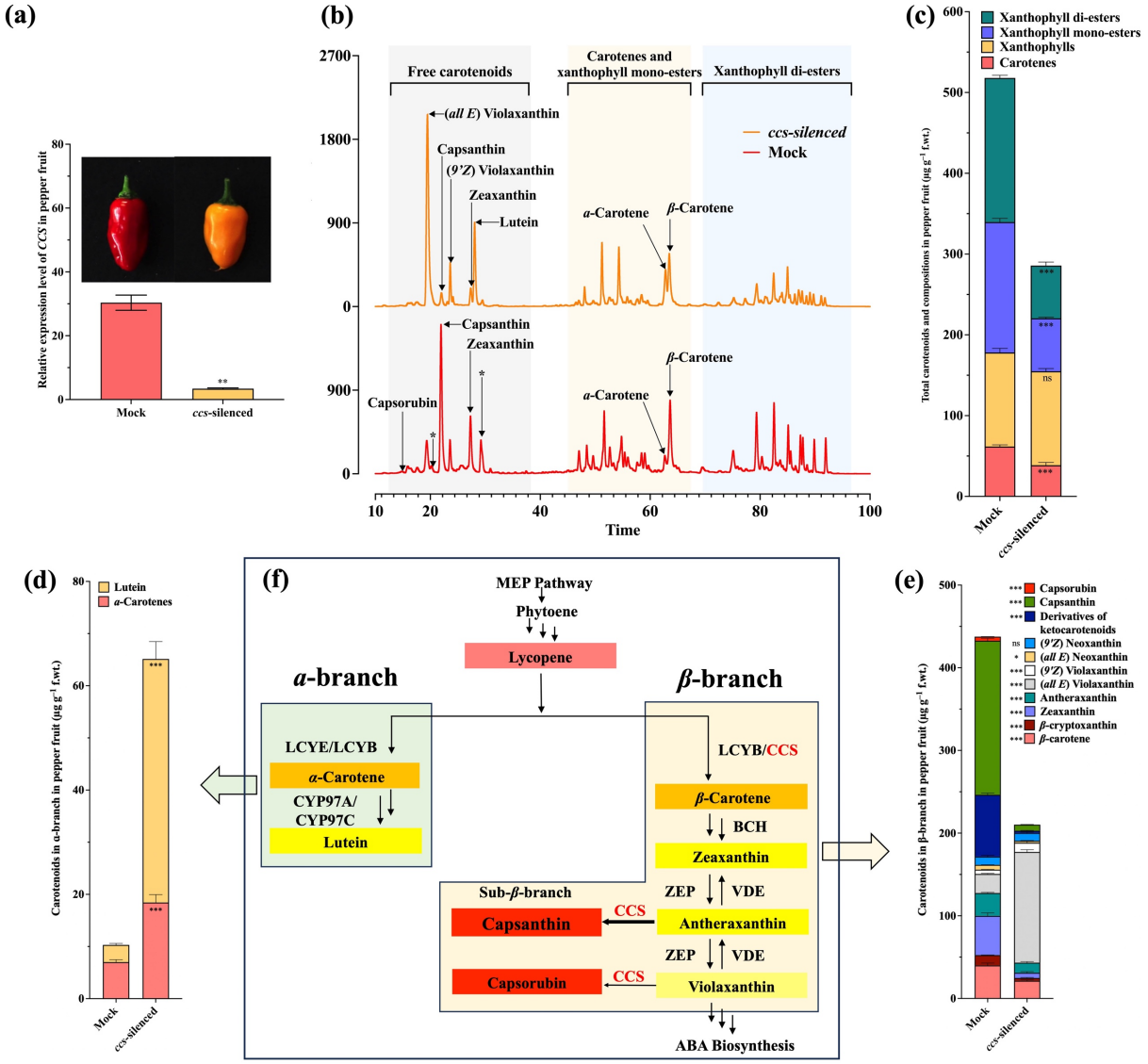

Figure 1. Characterizing the role of capsanthin/capsorubin synthase (CCS) in pepper. (a) The phenotype of *ccs*-silenced pepper fruit and relative expression level of *CCS* gene in *ccs*-silenced pepper fruits compared to mock-treated. Mock treatment refers to the pepper plants infected with VIGS-empty vector without harboring the gene sequence of interest (*CaCCS*). Data of quantitative RT-qPCR are presented as mean ± standard deviation of four biological replicates and three technical replicates. An unpaired t-test was performed (*: P<0.05; **: P <0.01). (b) HPLC chromatograms of mock or *ccs*-silenced pepper fruit carotenoids through the VIGS system. HPLC analyses were performed without saponification. '*' indicated the derivatives of capsanthin and capsorubin (Kim *et al.*, 2009). (c) Total carotenoids and their compositions in

937 pepper fruit. HPLC analyses were performed without saponification. (d–e) Carotenoid
938 compositions in the mock or *ccs*-silenced pepper fruits pepper fruit determined after
939 saponification. Data are presented as mean ± standard deviation of four biological replicates.
940 Two-way ANOVA was performed followed by Šídák's multiple comparisons test (*: P<0.05; **:
941 P<0.01; ***: P<0.001). (f) The carotenoid pathway in plants. The precursor, geranylgeranyl
942 diphosphate, is synthesized from the methylerythritol 4-phosphate (MEP) pathway. Phytoene
943 synthase (PSY) is the first committed step leading to the carotenoid phytoene. Lycopene is
944 synthesized from phytoene after multiple steps, including desaturation and isomerization.
945 Subsequently, lycopene is converted into *a*-carotene or *β*-carotene forming two sub-branches, *a*-
946 and *β*-branches in the following steps, highlighted in green and yellow color backgrounds,
947 respectively. In the *β*-branch, the specific steps in red pepper fruit, produce specialized
948 ketocarotenoids, capsanthin and capsorubin, to generate the sub-β-branch. LCYB, lycopene *β*-
949 cyclase; LCYE, lycopene *a*-cyclase, CYP97A/C, cytochrome P450-type monooxygenase 97A/C;
950 BCH, *β*-carotene hydroxylase; ZEP, zeaxanthin epoxidase; the sub-β-branch indicate the
951 carotenoid flow in pepper fruit.

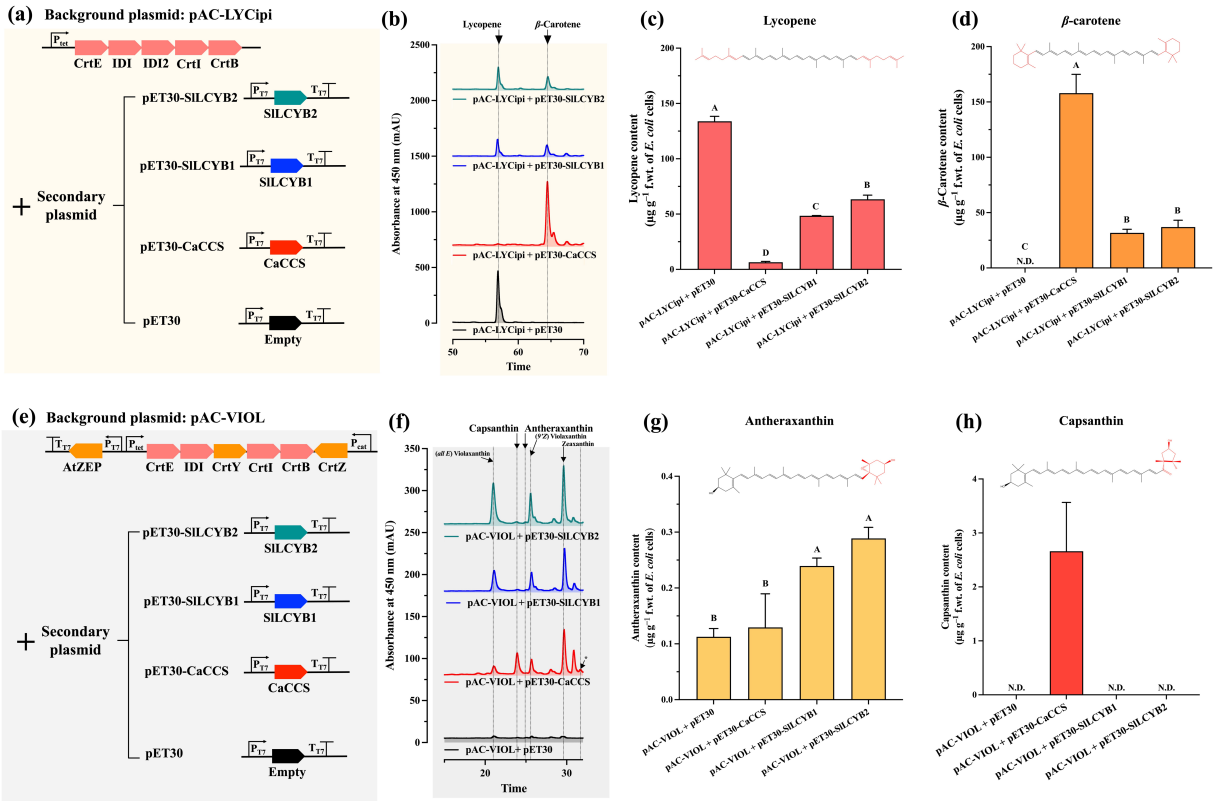

Figure 2. Functional validation and comparison of tomato LCYBs and pepper CCS in *E coli*. a. Schematic representation of different plasmid combinations used for lycopene and *β*-carotene production in *E. coli* cells. The *E. coli* strain, SixPack, harboring the background plasmid, pAC-LYCipi, can produce lycopene. A secondary plasmid containing tomato LCYB1, LCYB2, or pepper CCS was co-transformed with pAC-LYCipi in SixPack. b. The corresponding HPLC chromatograms to the pAC-LYCipi with pET30 (Empty vector), pET30-CaCCS, pET30-SlLCYB1, or pET30-SlLCYB2, respectively. Lycopene (c) and *β*-carotene (d) contents in SixPack harboring different plasmid combinations. e. Schematic representation of different plasmid combinations used for xanthophyll production in *E. coli* cells. The *E. coli* strain, SixPack, harboring another background plasmid, pAC-VIOL, can produce zeaxanthin without IPTG induction and violaxanthin with IPTG induction. Similar as (a), a secondary plasmid containing tomato LCYB1, LCYB2, or pepper CCS was co-transformed with pAC-VIOL in *E. coli*. f. The corresponding HPLC chromatograms to the pAC-VIOL with pET30 (Empty vector), pET30-CaCCS, pET30-SlLCYB1, or pET30-SlLCYB2, respectively. '*' indicated the derivatives of ketocarotenoids. Antheraxanthin (g) and capsanthin (h) contents in SixPack

968 harboring different plasmid combinations. The carotenoid contents were calculated using the
969 peak area of the HPLC chromatogram against standards, which are expressed as μg per gram
970 fresh weight of *E. coli* cells. Data of c–d and g–h are presented as mean ± standard deviation of
971 three biological replicates based on data from HPLC analyses. One-way ANOVA was performed,
972 followed by a mean separation test using the Tukey test and means significantly different at $p =$
973 0.05 are shown with different letter codes.
974

975

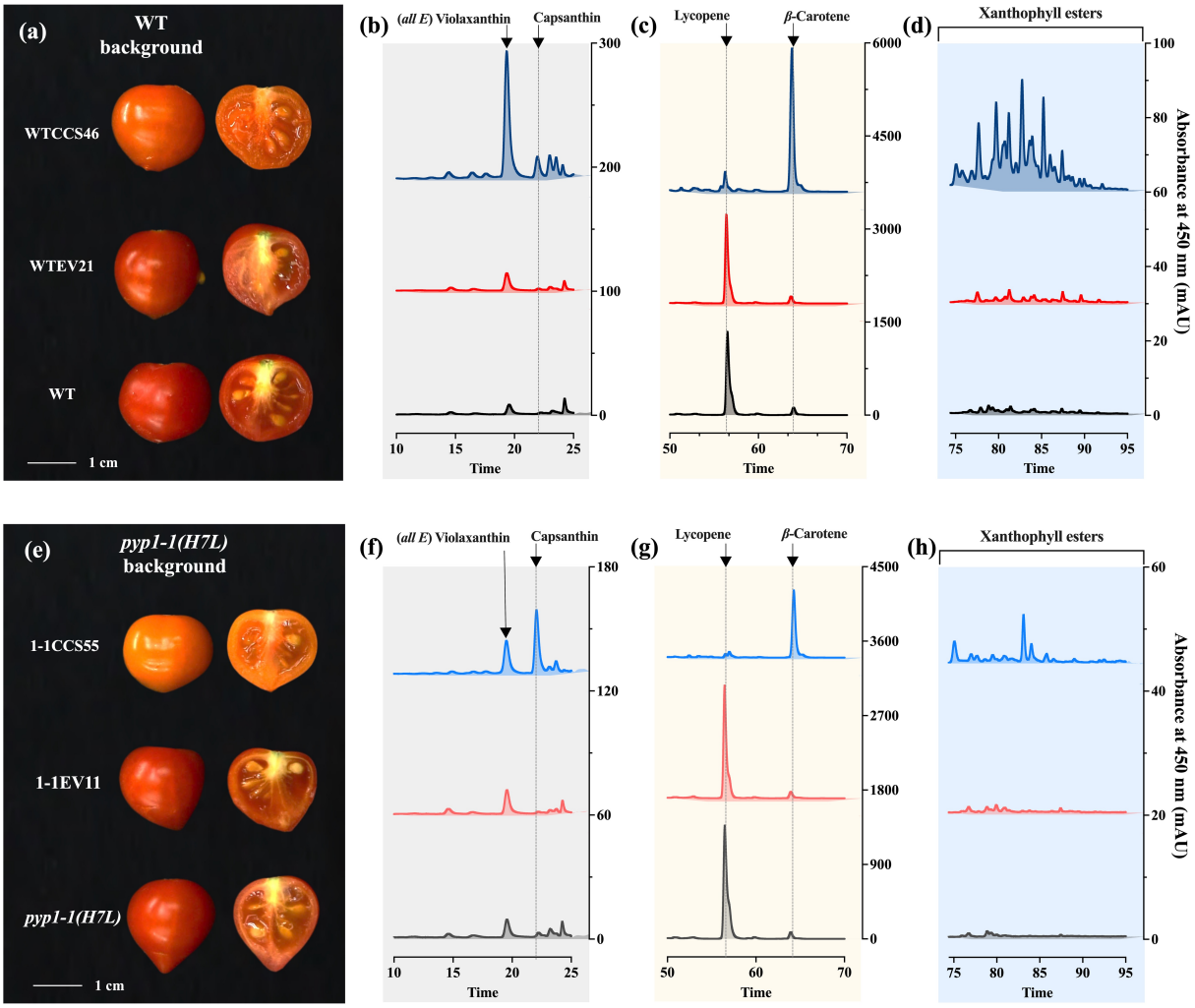

976

977 **Figure 3**. Phenotypes and carotenoid profiles of tomato fruit. Overexpression of pepper *CCS* was
978 performed in 'Micro-Tom' background, including two genotypes, wildtype (WT) (a–d) and *pyp1-*
979 *1(H7L)* mutant for an acyltransferase known in xanthophyll esterification (e–h). (a) The
980 phenotypes of tomato fruits from 'Micro-Tom' WT, 'Micro-Tom' transformed with empty vector,
981 WTEV21, and a representative line, WTCCS46, from multiple independent *CCS*-transformed
982 lines in 'Micro-Tom' WT background. (b–d) The corresponding HPLC chromatograms to 'Micro-
983 Tom' WT, WTEV21, and WTCCS46 lines. (e) The phenotypes of tomato fruits from 'Micro-Tom'
984 mutant, *pyp1-1(H7L)*, *pyp1-1(H7L)* transformed with empty vector, 1-1EV11, and a
985 representative line, 1-1CCS55, from multiple independent *CCS*-transformed lines in *pyp1-*

986 *1(H7L)*, background. (f–h) The corresponding HPLC chromatograms to 'Micro-Tom' mutant,
987 *pyp1-1(H7L)*, 1-1EV11, and 1-1CCS55.

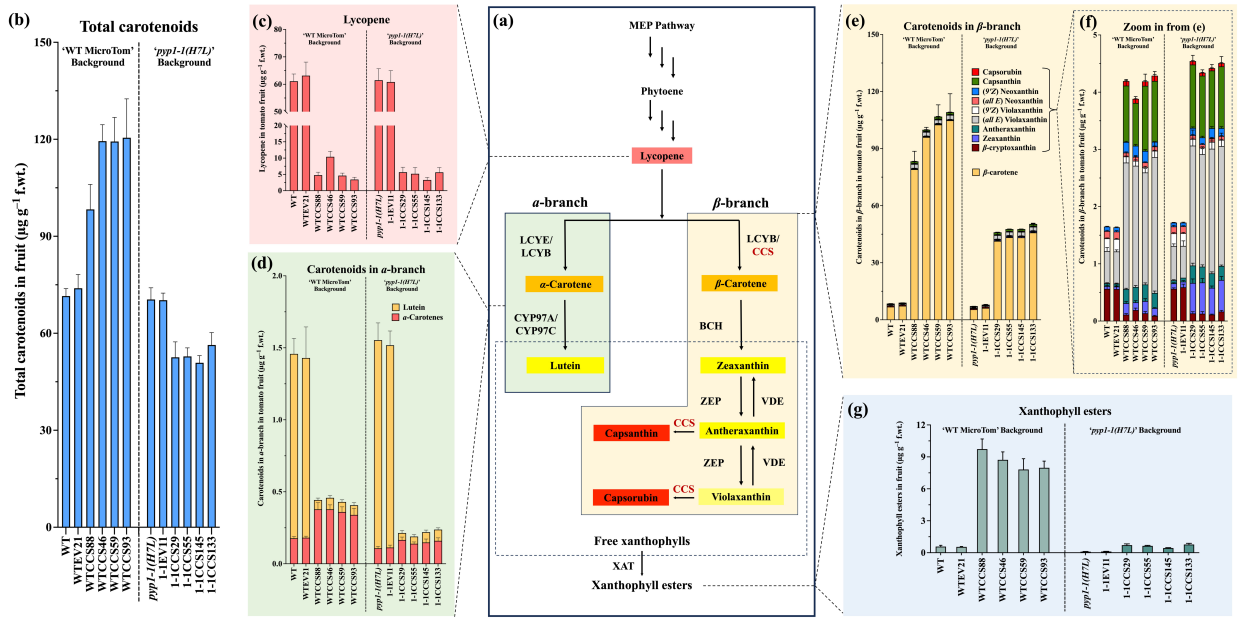

Figure 4. Compositional alterations in the carotenoid profiles of tomato in *CCS*-transformed tomato. (a) The carotenoid pathway in plants is listed in the black box at the center of this figure. Two branches, *α* and *β*-branch, are highlighted in green and yellow backgrounds. The xanthophylls in the dash-line box were available to be esterified under the catalysis of xanthophyll acyltransferase (XAT). Total carotenoids (b) and lycopene contents (c) in the fruit of control and independent *CCS*-transgenic lines in both WT 'Micro-Tom' and *pyp1-1(H7L)* backgrounds. (d) Carotenoid compositions, including lutein and *α*-carotene, in the *α*-branch of carotenoid pathway. (e) Carotenoid compositions, including *β*-carotene, *β*-cryptoxanthin, zeaxanthin, antheraxanthin, violaxanthin, neoxanthin, capsanthin and capsorubin in the *β*-branch of carotenoid pathway. (f) A zoom-in view of carotenoids in *β*-branch from (e) except for *β*-carotene. (g) Xanthophyll esters in the fruit of control and independent *CCS*-transgenic lines in both WT 'Micro-Tom' and *pyp1-1(H7L)* backgrounds. Data of b–g are presented as mean ± standard deviation of a minimum of four biological replicates based on data from HPLC analyses. One-way ANOVA was performed followed by mean separation test using the Tukey test (*: P<0.05; **: P<0.01; ***: P<0.001), details of which are shown in the supplementary Excel file.

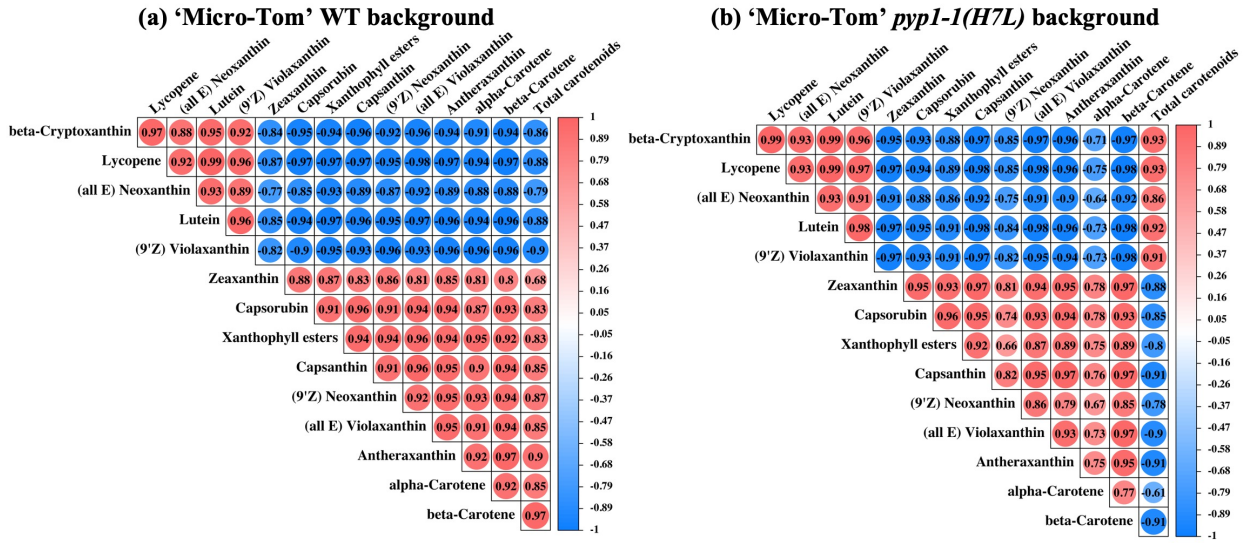

Figure 5. Pearson correlation matrix between each paired carotenoid levels analyzed from ripe tomato fruit. The Pearson correlation coefficient of each paired carotenoid composition is shown in each cell computed based on the carotenoid contents from the set of WT, WTEV and WTCCS lines (a), or *pyp1-1(H7L)*, 1-1EV, and 1-1CCS lines (b) using a R package 'corrplot'. The Pearson correlation coefficient shown in the cell indicates that it was tested significantly (p-value <0.05), while a tested insignificant correlation would not be shown in the cell. The color intensity and the size of each circle indicated the strength of correlation between each paired carotenoids, in which the more intense the color and larger the circle size are, higher the correlation between each paired carotenoids is. Red indicates positive correlations and blue indicates negative correlations.

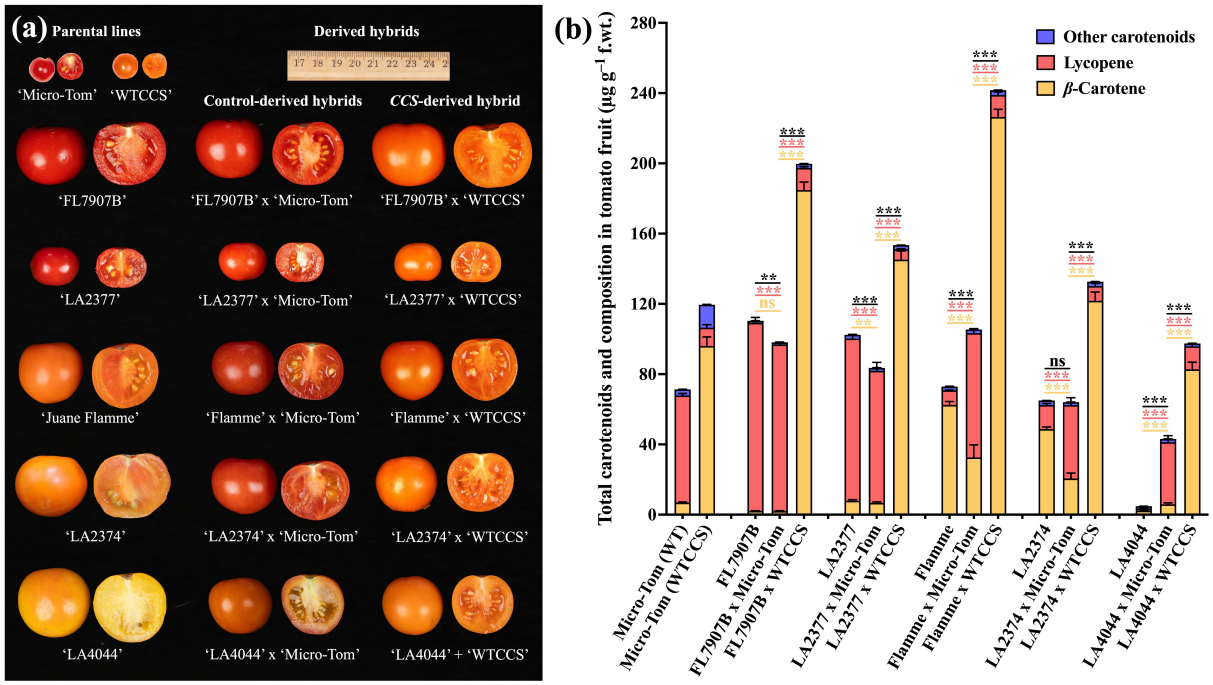

Figure 6. Phenotypic characterization of ripe fruit and carotenoid compositions of parental lines, control- and *CCS*-derived F1 hybrids. (a) Phenotypes of ripe fruit from parental lines, control- and *CCS*-derived hybrids. Five tomato inbred lines, 'FL7907B', 'LA2377', 'LA2374', 'Jaune Flamme', and 'LA4044', were selected as maternal lines. The transgenic line, WTCCS46, generated in this study and 'Micro-Tom' (WT background) were used as paternal lines. (b) Total carotenoids and their compositions in the fruit of parental lines, control- and *CCS*-derived F1 hybrids. Data are presented as mean ± standard deviation of a minimum of four biological replicates based on HPLC analyses. One-way ANOVA was performed followed by mean separation using the Tukey test (*: P<0.05; **: P<0.01; ***: P<0.001). The asterisk color, yellow, pink, and black indicate the mean comparisons of *β*-carotene, lycopene, and total amounts of carotenoids, respectively.

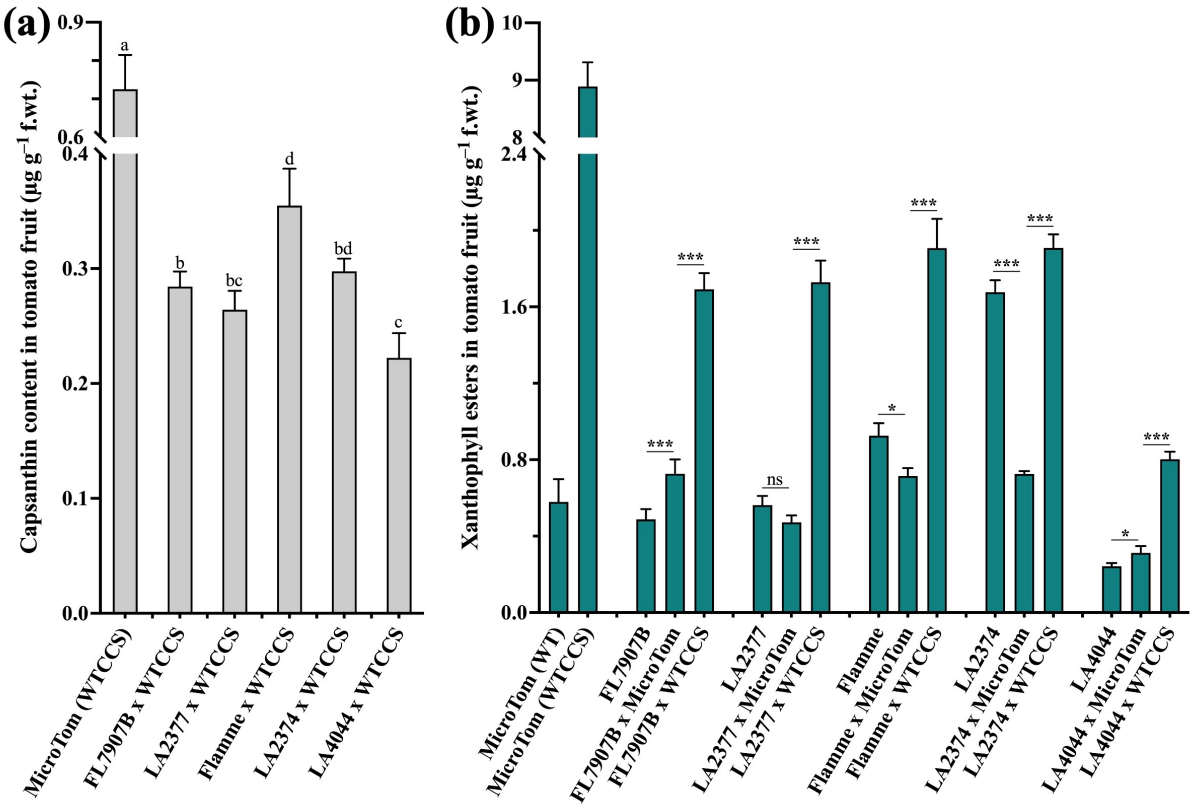

Figure 7. Contents of capsanthin (a) and xanthophyll esters (b) in the fruit of control- and *CCS*-derived hybrids. Data are presented as mean ± standard deviation of a minimum of four biological replicates based on HPLC analyses. One-way ANOVA was performed followed by mean separations using the Tukey test (*: P<0.05; **: P<0.01; ***: P<0.001).

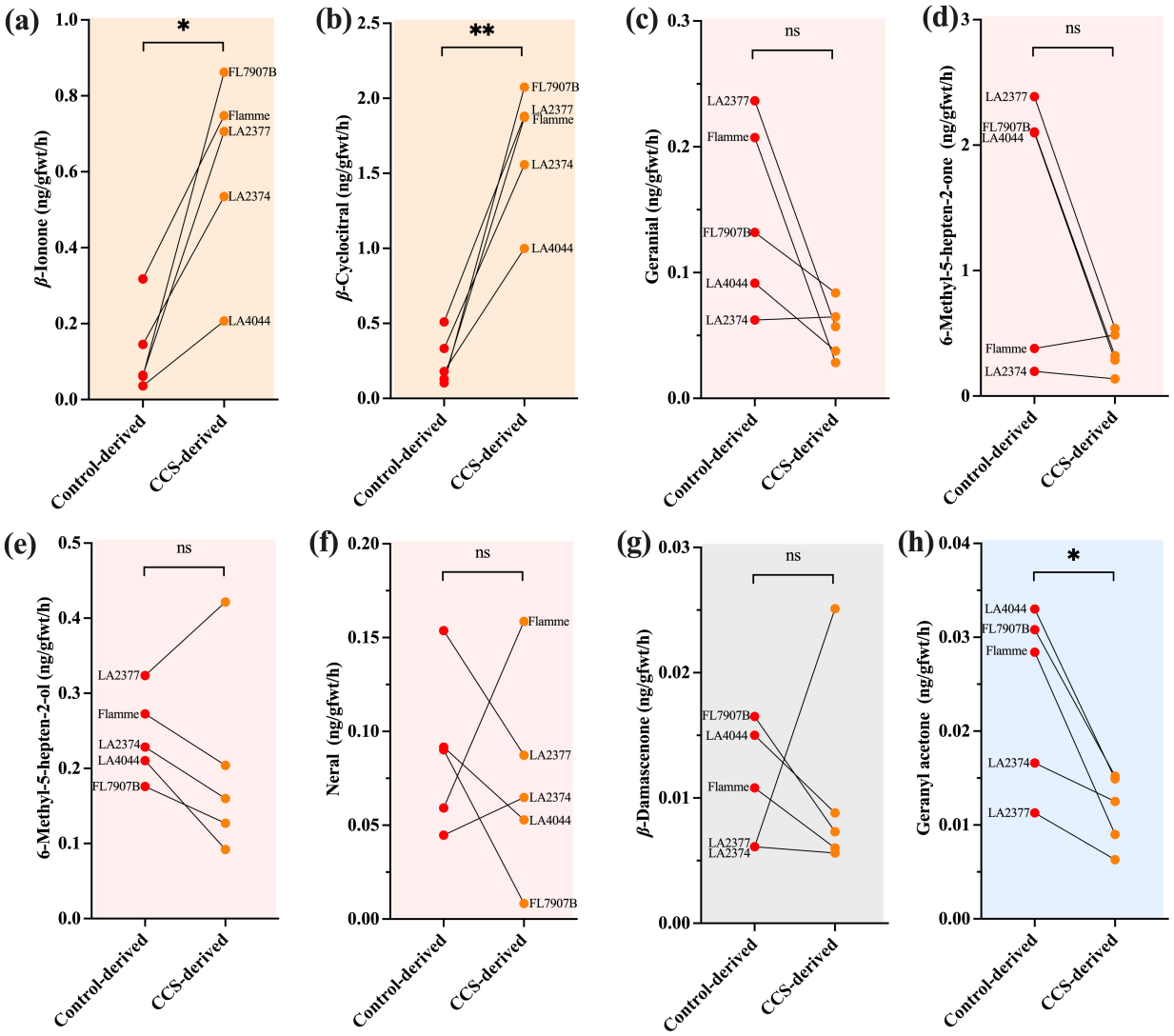

Figure 8. Volatile apocarotenoid derived from carotenoids in ripe tomato from control and CCS-derived hybrids. Beta-ionone (a) and *β*-cyclocitral (b) are derived from *β*-carotene, highlighted in orange background. Geranial (c), 6-methyl 5-hepten-2-one (d), 6-methyl 5-hepten-2-ol (e), and neral (f) are derived from lycopene, highlighted in red background. Beta-damascenone (g) and geranyl acetone (h) are derived from neoxanthin and phytoene respectively, highlighted in gray and blue backgrounds respectively. Data are from 100 g fruit for each plant analyzed by individual runs of GC-MS. 'FL7907B', 'LA2377', 'Flamme', 'LA2374', and 'LA4044' represent the maternal lines crossed with WT 'Micro-Tom' (red dots) or 'WTCCS' (orange dots). Asterisks indicate significant (*, $p<0.05$) or highly significant (**, $p<0.01$) differences following

1043 a paired T-test between the control-derived hybrid group and *CCS*-derived hybrid group (n=5).

1044 NS – No significant difference.

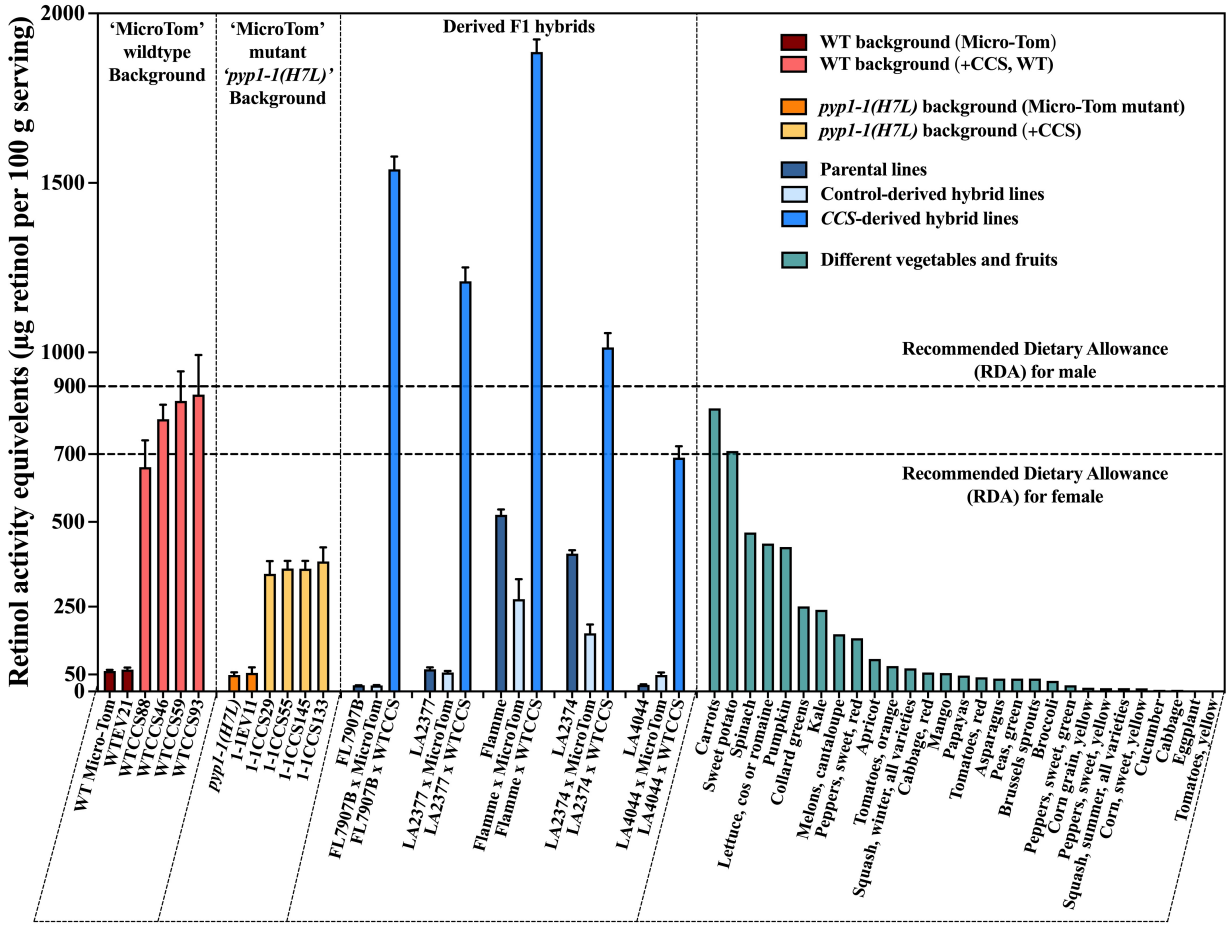

Figure 9. Retinol activity equivalents (RAE) in different vegetables and fruits. RAE values were computed based on the contents of provitamin A, including *β*-carotene, *β*-cryptoxanthin, and *a*-carotene in tomato fruit of engineered lines in this study. The RAE values from different vegetables and fruits, including common sources, were grouped into four, distinguished by dash lines in the figure. The first group depicts data for engineered tomato lines with 'Micro-Tom' WT background. The second group contains engineered tomato lines under the 'Micro-Tom' *pyp1-1(H7L)* mutant background. The third group contains the parental lines and their derived F1 hybrids. The parental lines included WT 'Micro-Tom' and 'WTCCS Micro-Tom' (paternal) and five selected inbreds (maternal) 'FL7907B', 'LA2377', 'Juane Flamme', 'LA2374', and 'LA4044'. The fourth group referred to the RAE values of different vegetables and fruits collected from the USDA database (standard reference legacy), whose details are listed in a supplementary Excel file.

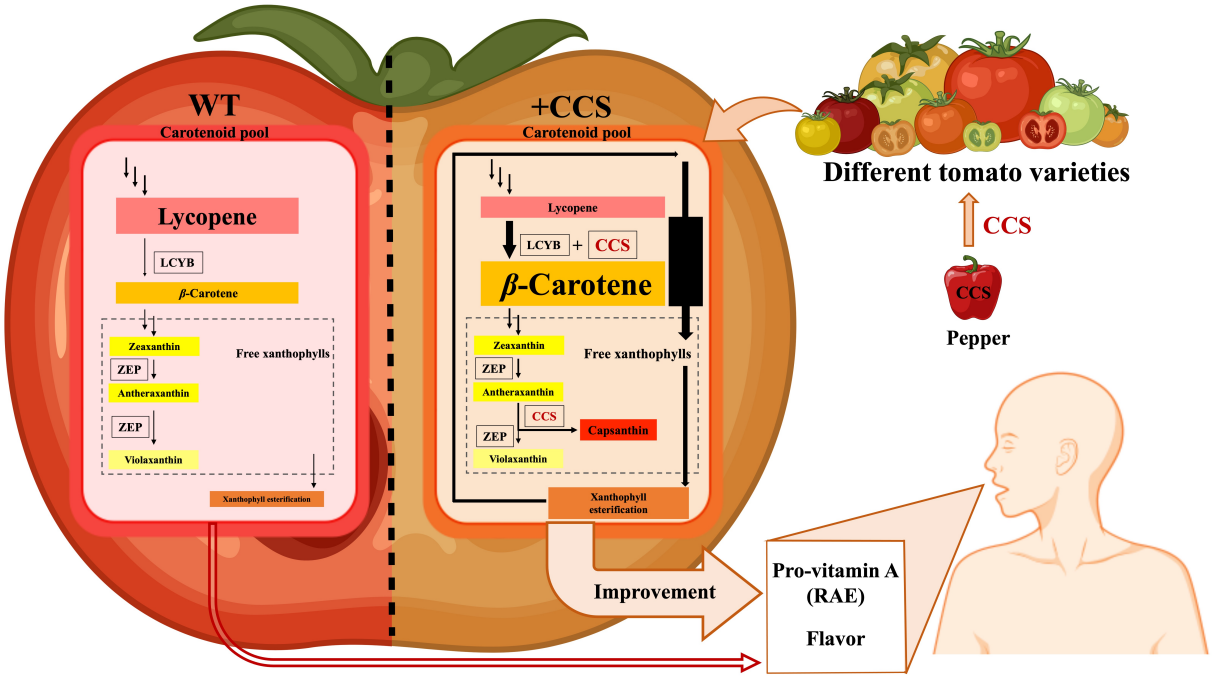

Figure 10. Schematic representation of phenotypic and metabolic alteration in *CCS*-transformed tomato fruit. The carotenoid pathway in WT tomato fruit is shown on the left. The altered carotenoid pathway by overexpression of pepper *CCS* in tomato fruit is shown on the right. The size of the arrow and each carotenoid represent the relative flux size and metabolite abundance in the pathway. Both pathways are shown in the presence of the xanthophyll esterification process. The accumulation of xanthophyll esters, highlighted in orange box, was positively correlated with the amounts of total carotenoids, *β*-carotene and other carotenoids, indicating its ability to facilitate carotenoid biosynthesis when *CCS* was overexpressed. Overexpression of pepper *CCS* in different tomato varieties (represented here with different color tomatoes), contributed to metabolic alterations of the carotenoid pathway and remarkably enhanced biofortification of provitamin A (*β*-carotene) for human nutrition. LCYB, lycopene *β*-cyclase; ZEP, zeaxanthin epoxidase; CCS, capsanthin/capsorubin synthase, highlighted in red. Design components of the figure were obtained from 'BioRender' and further assembled in PowerPoint.

Supplementary Figures and Tables

Capsanthin/Capsorubin Synthase Expression in Tomato Alters Carotenoid Pools, Enhancing Provitamin A and Flavor Volatiles

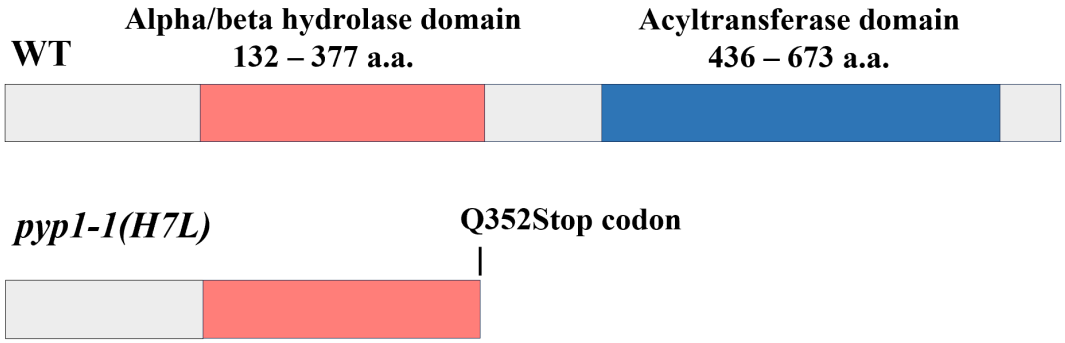

Figure S1. Protein structure of xanthophyll acyltransferase in WT 'MicroTom' (Top) and *pyp1-1(H7L)* mutant (bottom) in 'MicroTom' background. A non-sense mutation occurred at the 352nd amino acid residue, causing a stop codon and a complete loss of the acyltransferase domain. Domain lengths are drawn not proportional to sequence length.

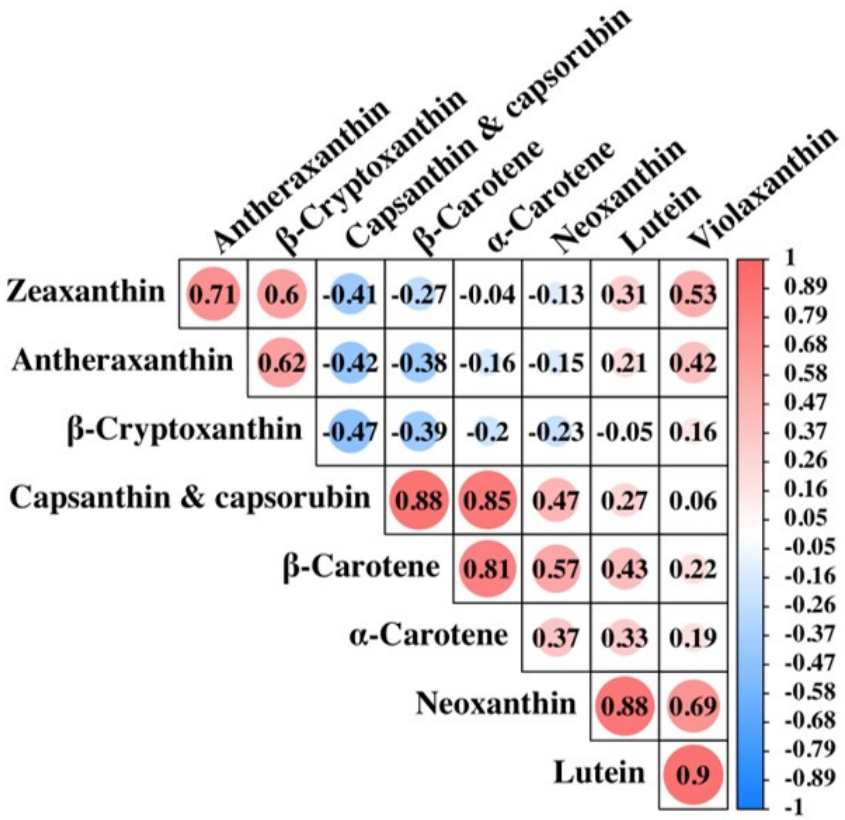

Figure S2. Pearson correlation matrix between each paired carotenoid content analyzed from ripe fruit of 32 pepper varieties. The data were from a previous study Wahyuni et al., (2011) and re-analyzed here. The color intensity and the size of each circle in the chart indicated a higher correlation, in which red referred to positive correlations and blue to negative correlations.

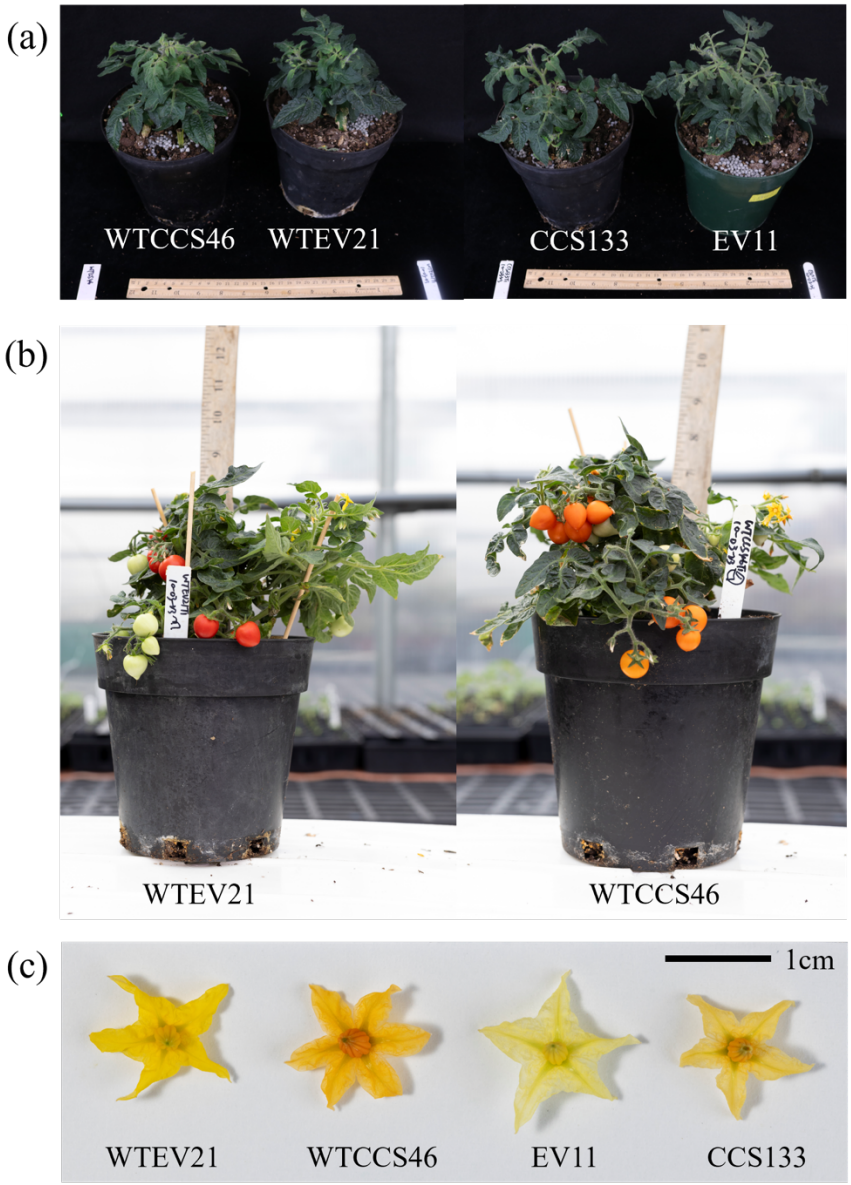

Figure S3. Plant growth and yield. Vegetative growth of Micro-Tom plants without or with transforming pepper *CCS* gene (a). Reproductive stage of Micro-Tom plants without or with transforming pepper *CCS* gene (b). The flower color of Micro-Tom plants without or with transforming pepper *CCS* gene (c).

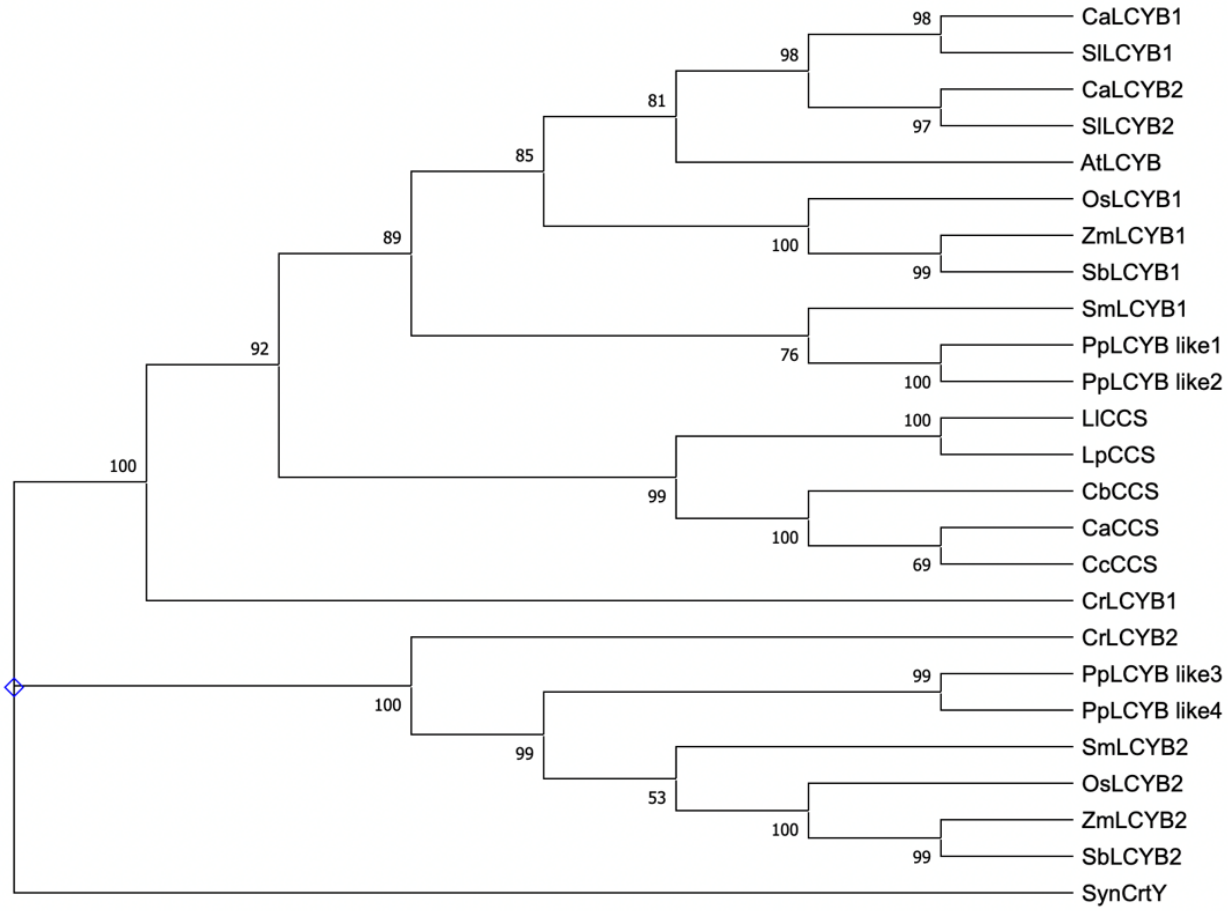

Figure S4. Phylogram of capsanthin/capsorubin synthase (CCS) and lycopene β-cyclase (LCYB) protein sequences. Phylogenetic analysis of CCS and LCYB protein sequences from different plant species. The rooted phylogenetic tree was generated by MEGA 11.0. CCS and LCYB protein sequences were aligned with MUSCLE program and then were constructed using the Maximum Likelihood method. The bootstrap values shown on the nodes were computed from 1000 replicates. CCS protein sequences were from *Capsicum annuum* (Ca, NP_001311998.1, Capana06g000615, CA06g22860), *Capsicum chinense* (Cc, PHU16032.1), and *Capsicum baccatum* (Cb, PHT30120.1), *Lilium lancifolium* (Ll, PHT30120.1), *Lilium pumilum* (Lp, AQZ41157.1). The LCYB protein sequence were from dicot: *Capsicum annuum* (CaLCYB1: XP_016543793; CaLYCB2: NP_001311908), *Solanum lycopersicum* (SlLCYB1: Solyc10g079480.1, XP_010312096; SlLCYB2: Solyc04g040190.1, NP_001234226), and *Arabidopsis thaliana* (AtLCYB, AT3G10230.1, NP_001078131); monocot: *Oryza sativa* (Os, OsLCYB1, XP_066163296.1; OsLCYB2, XP_015622198.1), *Zea mays* (Zm, ZmLCYB1, NP_001169155.1; ZmLCYB2, NP_001146840.1), Sorghum bicolor (SbLCYB1, XP_002453448.1; SbLCYB2, XP_002455838.1); moss: *Physcomitrella patens* (PpLCYB like1, XP_024371653.1; PpLCYB like2, XP_024373649.1; PpLCYB like3, XP_024389432.1; PpLCYB like4, XP_024380943.1); gymnosperm: *Selaginella moellendorffii* (SmLCYB1, XP_002971295.2; SmLCYB2, XP_002974344.1); Algae: *Chlamydomonas reinhardtii* (CrLCYB1, XP_042921724.1; CrLCYB2, XP_001696529.1); Cyanobacteria: *Synechococcus* sp. PCC 7335 (SynCrtY, WP_006454809.1

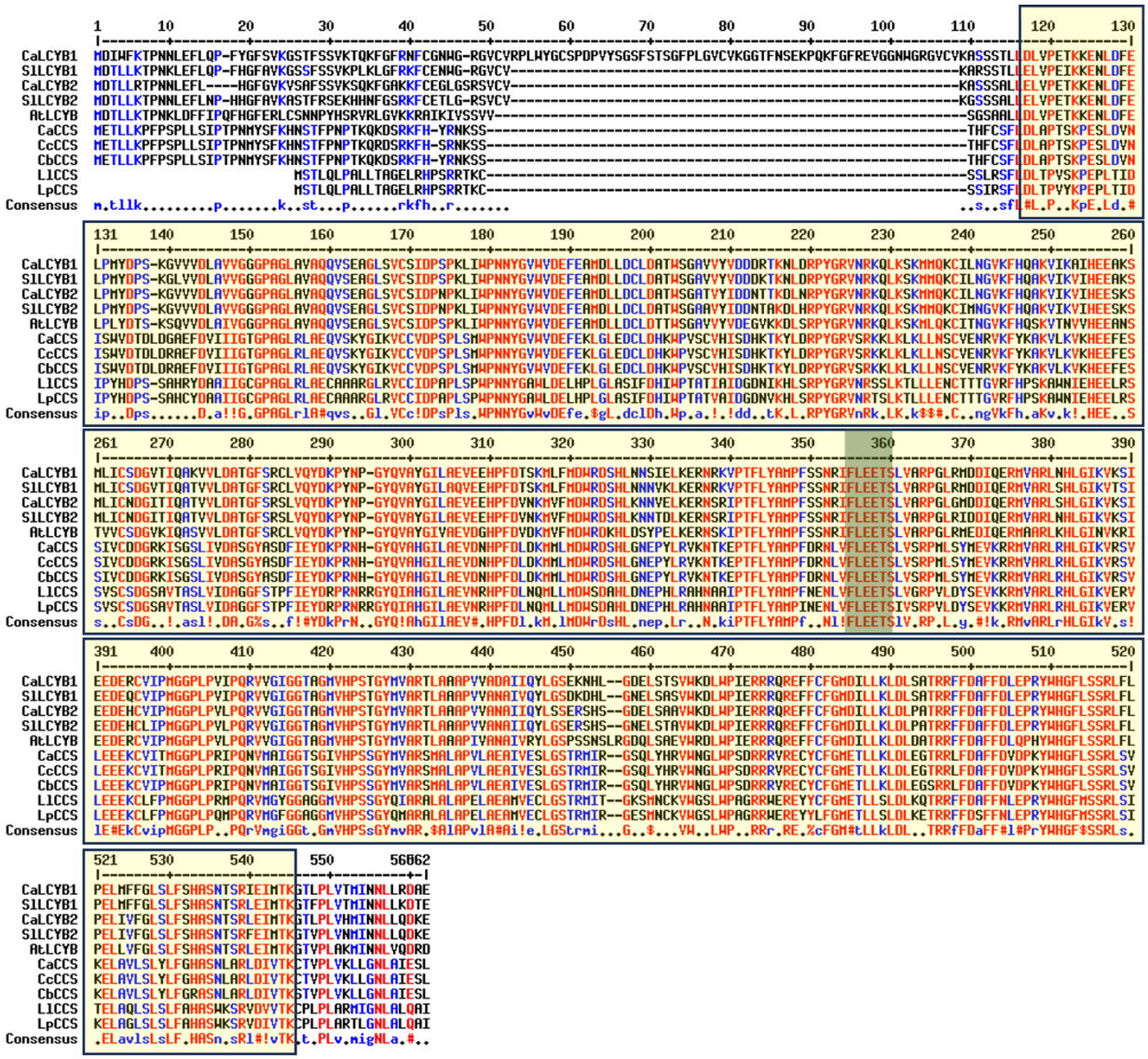

Figure S5. Alignment of CCS and LCYB protein sequences using MultaAlin (Corprt, 1988; http://multalin.toulouse.inra.fr/multalin/). Identical amino acids from all protein sequences were highlighted in red color. Low consensus amino acid residues from all protein sequences were highlighted in blue color. Except for CCS protein sequences mentioned in A, LCYB protein sequences were from *Capsicum annuum* (CaLCYB1: Capana10g002320, CA10g20140, XP_016543793; CaLYCB2: Capana05g000023, CA05g00080, NP_001311908), *Solanum lycopersicum* (SlLCYB1: Solyc10g079480.1, XP_010312096; SlLCYB2: Solyc04g040190.1, NP_001234226), and *Arabidopsis thaliana* (AtLCYB: AT3G10230.1, NP_001078131). The deduced amino acid sequences of CCS and LCYB contained a lycopene cyclase domain by InterPro (Paysan-Lafosse et al., 2023) and are highlighted in a yellow box. The active motif, FLEET, is highlighted in a green box.

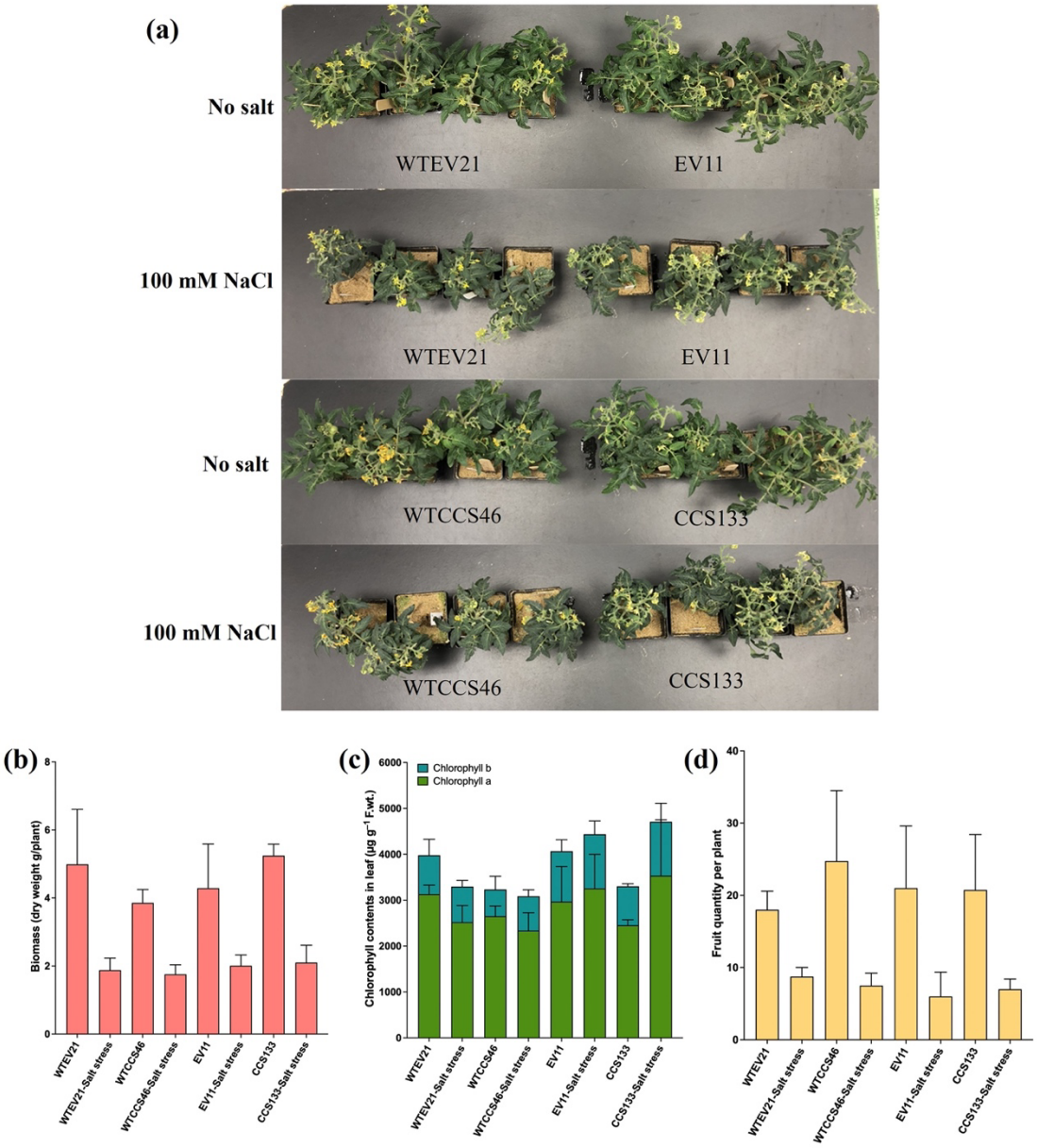

Figure S6. Evaluation of plant growth and salinity tolerance**.** Plant growth (a), plant biomass (b), chlorophyll contents (c), and fruit quantity (d) after treated with or without 100 mM NaCl. One-month-old seedlings of empty vector and *CCS*-transformed lines in Micro-Tom background or Micro-Tom *pyp1-1(H7L)* mutant background were chosen for this test. Four replicate plants at 4-5 leaf stage were transplanted in 0.5L-capacity plastic containers filled with fine vermiculite. The plants were kept under a light bench (120 µmoles.m^2,16h light/8 h dark, 25°C/23 °C) and irrigated two pot volumes, six days per week, using half-strength Hoagland nutrient medium (pH=6.0) for control plants or with the same medium with 10 mM $CaCl_2$ and NaCl (100 mM final strength, step-wise increased by 50 mM NaCl every three days and kept at 100 mM NaCl). Plants were photographed during flowering. The plants were grown for 3.5 months until the harvest of ripe fruit. Total above-ground biomass (dry weight) and fruit numbers were collected. We have not observed any developmental impacts due to CCS overexpression other than the

changes in the flower and fruit color. In an experiment on container-grown plants supplied with a half-Hoagland nutrient medium, the biomass and fruit numbers were not significantly different between the vector control and CCS-overexpressing line in both wild-type and *pyp1-1(H7L)* mutant background. Also, based on biomass and fruit numbers, CCS-overexpressing lines did not have an advantage under salinity stress induced by 100 mM NaCl.

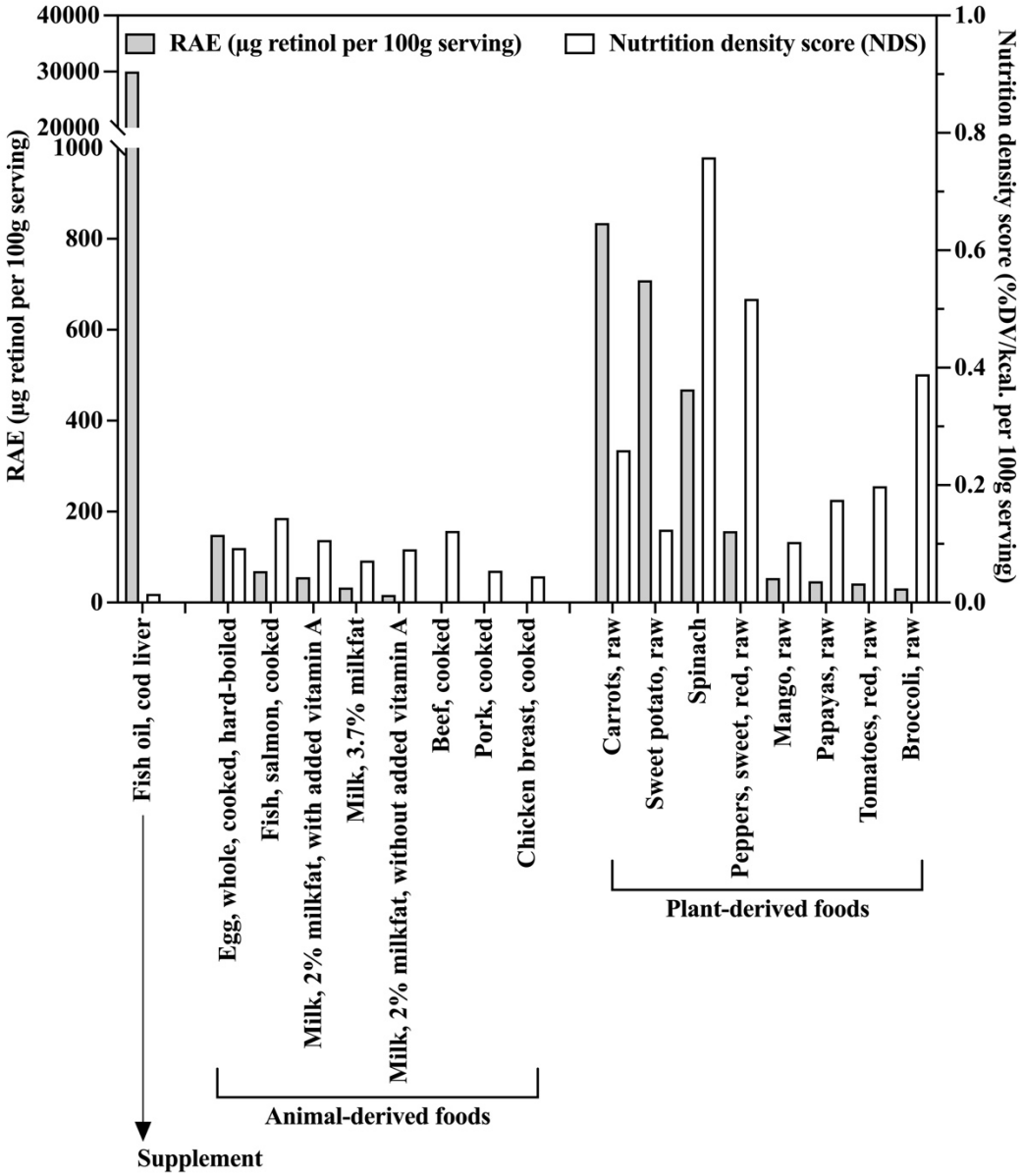

Figure S7. Retinol activity equivalents and nutrient density scores from multiple food sources. The data were obtained from the USDA database (standard reference legacy), the details of which were listed in a supplementary Excel file. The nutrient density scores were computed based on the method reported by Pampersaud et al., (2012).

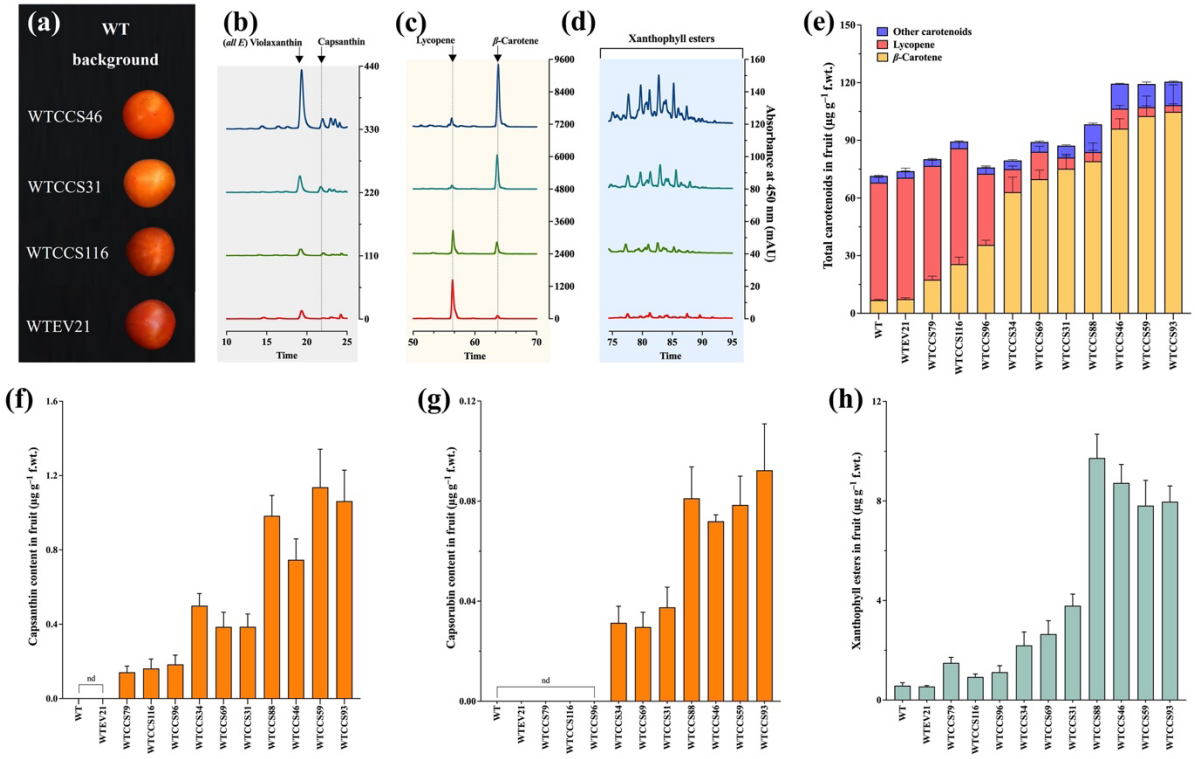

Figure S8. Phenotypes of the fruit from independent *CCS*-overexpression lines of tomato and their carotenoid compositions. Overexpression of pepper *CCS* was performed in 'MicroTom' background, including two genotypes, wildtype (WT) and *pyp1-1(H7L)* mutant for an acyltransferase defective in xanthophyll esterification. Additional independent lines potentially differing in their expression level of CCS in 'MicroTom' WT background were screened and analyzed. The data of WTCCS line 88, 46, 59, 93, are shown in Fig. 2 and Fig. 3, are included for comparison purposes. a. The phenotypes of tomato fruits from 'MicroTom' and independent *CCS*-transgenic lines in WT 'MicroTom' background. The fruits of independent *CCS*-transgenic lines, WTCCS116, WTCCS31 and WTCCS46, were chosen to represent low (lines 79, 116, and 96), medium (lines 34, 69, and 31), and high- (line 88, 46, 59, and 93) types classified based on fruit color and the PCA analysis on their carotenoid compositions (Fig. S6). b–d. The corresponding HPLC chromatograms to the representative fruit shown in a (WT 'MicroTom' background). Total carotenoids and their compositions (e), capsanthin (f), capsorubin (g), and total xanthophyll esters (h), in the fruit of independent *CCS*-transgenic lines in 'MicroTom' WT background. Data of I–L are presented as mean ± standard deviation of a minimum of four biological replicates based on data from HPLC analyses. One-way ANOVA was performed followed by mean separations using the Tukey test (*: P<0.05; **: P<0.01; ***: P<0.001), the details of which are shown in the supplementary Excel file.

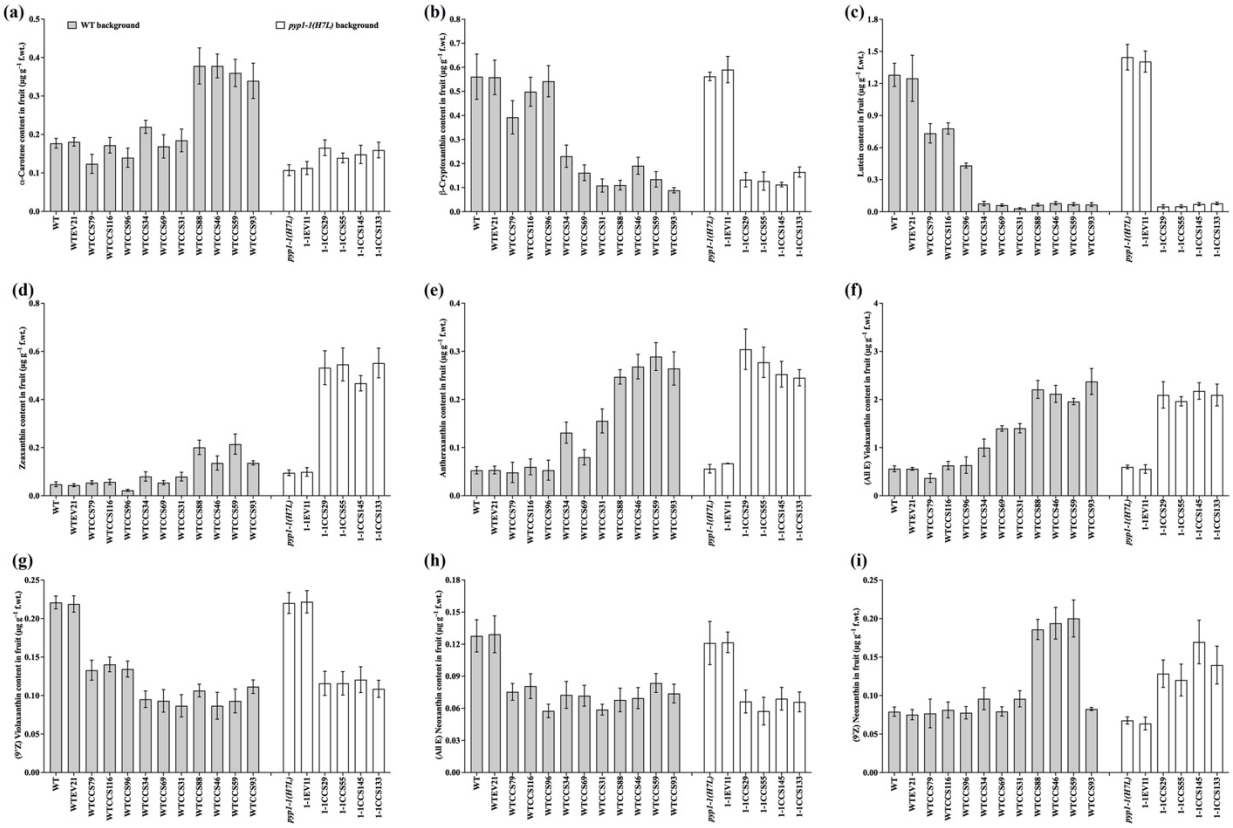

Figure. S9. Carotenoids in the fruit of independent *CCS*-transgenic lines in 'MicroTom' background. Overexpression of pepper *CCS* was performed in 'MicroTom' background, including two genotypes, wildtype (WT) and *pyp1-1(H7L)* mutant for an acyltransferase defective in xanthophyll esterification. Multiple independent lines with different potential expression levels of CCS in 'MicroTom' WT background were screened and analyzed. The data of WTCCS line 88, 46, 59, 93 and 1-1CCS line 29, 55, 145, 133 shown in Fig. 2 and Fig. 3, have been included here to facilitate comparisons. Alpha-carotene (a), β-cryptoxanthin (b), lutein (c), zeaxanthin (d), antheraxanthin (e), (*all E*) violaxanthin (f), (*9'Z*) violaxanthin (g), (*all E*) neoxanthin (h), (*9'Z*) neoxanthin (i). Data are presented as mean ± standard deviation of a minimum of four biological replicates based on HPLC analyses.

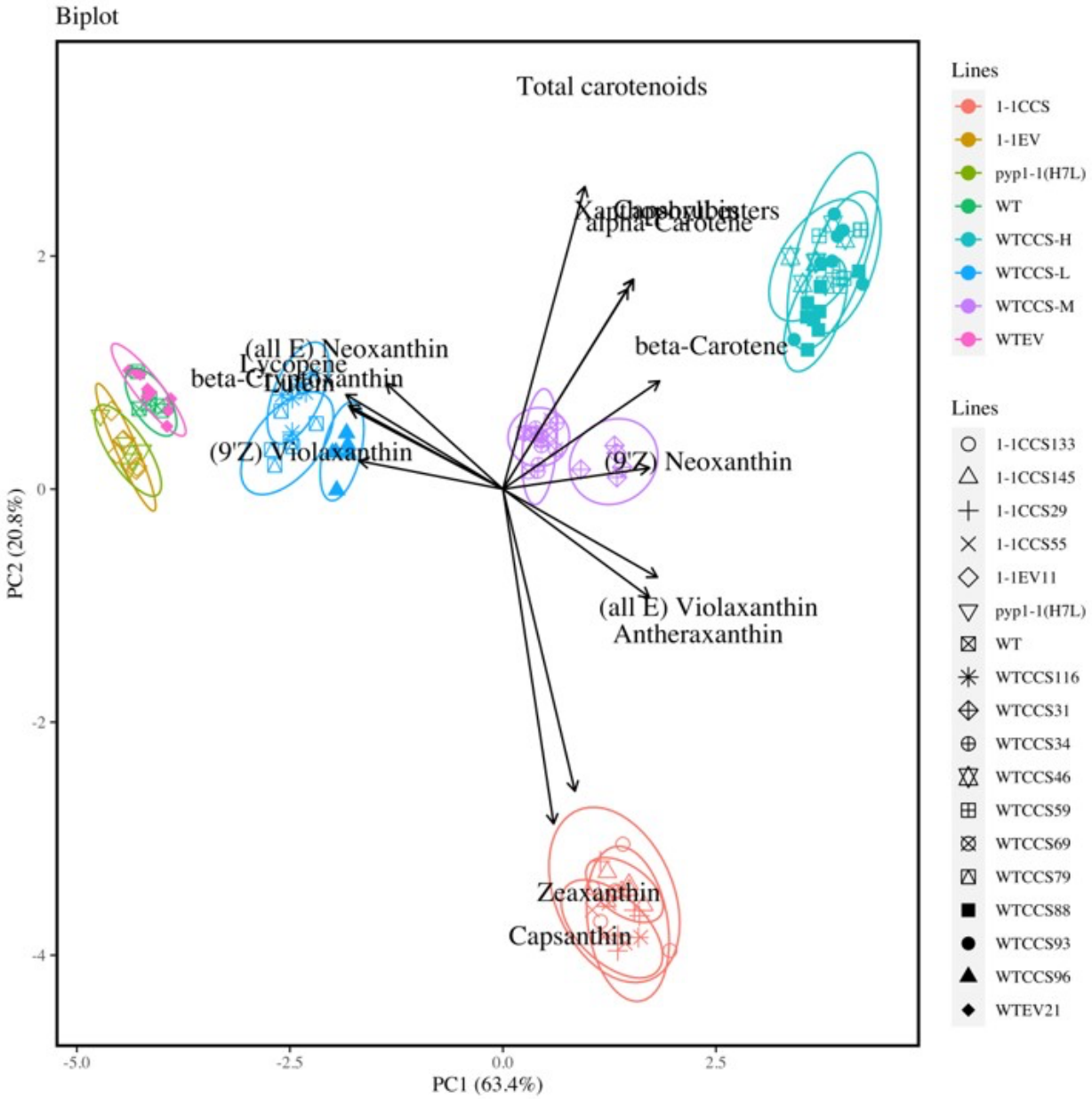

Figure S10. Biplot of principal component analysis (PCA) on carotenoid content in ripe tomato fruit of different *EV*- or *CCS*-transgenic lines [in both WT and *pyp1-1(H7L)* background]. PCA was performed based on the contents of carotenoids determined in fruits harvested from all lines including WT, *EV*-transformed WT, *CCS*-transformed WT, *pyp1-1(H7L)*, *EV*-transformed *pyp1-1(H7L)*, *CCS*-transformed *pyp1-1(H7L)*, which were shown in Fig. 3, Fig. S4 and Fig. S5. Biplot contained loadings, PC scores, and Proportion of variance.

Table S1. List of primers in this study.

Name of primer	Forward sequence (5’ to 3’)	Reverse sequence (5’ to 3’)
CaCCS full CDS	CACCAGTGATTCCCCTAGTTCGGTATT	AAGGCTCTCTATTGCTAGATTGC
CaCCS VIGS	AGGCCTCCATGGCCTTTTCCATCTCCTTTACTT	CCGGGCCTCGAGCTGTCCAAATACTTAGTCTTGTGAT
CaCCS qPCR	TACTGGCACGGGTTCCTTTC	TGCTAGATTGCCCAGCAGTT
CaUbCE qPCR	GAGCTCAAGGATCTGCAAAAGGA	GTTCTAAAAGCAACCTTTGGAGGC
CaCCS pET30	TATGGCAGATCTCAGCTTTCTTGATTTAGCACCCAC	ACCAGACTCGAGGCTCTCTATTGCTAGATTGCC
SlLCYB1 pET30	GAATTCGAGCTCCTTTTAGAGCTTGTACCTGAGACC	TCGAGTGCGGCCGCTCATTCTTTATCCTGTAACAAATTGTTGATCATAT
SlLCYB2 pET30	GAATTCGAGCTCCTTTTGGAGCTTGTACCTGAGATAAAG	TCGAGTGCGGCCGCTCATTCTGTATCCTTTAACAAATTGTTAATCATAG
Genotyping for transformation (promoter region)	GACCAAAGGGCTATTGAGAC	AAATACCGGAGTCCTCTCCA
Genotyping for transformation (CCS region)	TGGAGAGGACTCCGGTATT	AAGGCTCTCTATTGCTAGATTGC
SlSYS (Copy number)	GGAATTTAAACAGGGTGGAGTGTC	GGGGCTCTTGATATTGCTTTCAC
SlPDS (Copy number)	TCTTCATTGGACCTTTTGTGTGC	GCTTCAACATAAGATTGCCCTCC
CCS (Copy number)	GGATTCCATTGCCCAGCTATC	TTGCTTTGAAGACGTGGTTGG

Table S2. Medium for plant transformation. All media were adjusted to pH 5.7 prior to autoclaving. Plant growth regulators, antibiotic stocks, acetosyringone, and 2-mercaptoethanol, were filter-sterilized and added after autoclaving.

Medium	Components including antibiotics, plant growth regulators and so on
YEP medium	YEP medium containing 50 mg L^{-1} spectinomycin, 10 mg L^{-1} rifampicin, and 20 mg L^{-1} gentamycin
Preculture medium	MS medium supplemented with 3% (w/v) sucrose, 2 mg L^{-1} zeatin and 0.8% (w/v) agar
Co-cultivation medium	MS medium supplemented with 3% (w/v) sucrose, 2 mg L^{-1} zeatin, 100 μM acetosyringone, 10 μM 2-mercaptoethanol, and 0.8% (w/v) agar
Callus induction medium	MS medium supplementing with 3% (w/v) sucrose, 2 mg L^{-1} zeatin, 100 mg L^{-1} kanamycin, 100 mg L^{-1} timentin, 300 mg L^{-1} cefotaxime, and 0.8% (wt./v) agar
Shoot induction medium	MS medium supplemented with 3% (w/v) sucrose, 1 mg L^{-1} zeatin, 100 mg L^{-1} kanamycin, 100 mg L^{-1} timentin, 300 mg L^{-1} cefotaxime, and 0.8% (wt./v) agar
Rooting medium	0.5 x MS medium supplemented with 1.5% (w/v) sucrose, 1 mg L^{-1} IAA, 50 mg L^{-1} kanamycin, 100 mg L^{-1} timentin, 300 mg L^{-1} cefotaxime, and 0.6% (w/v) agar

Table S3. Chromatographic method.

Conditions	
Main column	Thermo Scientific Acclaim RSLC 120 C18 column (250 mm x 2.1 mm i.d., 2.2 μm)
Guard column	A similar material of main column (20 mm x 4.6 mm)
Temperature	35°C
Injection	1 μL
Flow rate	0.1 ml/min
Detector	The carotenoids were detected at a wavelength of 450 nm, and the spectra were acquired and processed using the ChemStation software.
Mobile phase	The mobile phase consisted of eluent A (water) and eluent B (acetone) using a gradient program as follows: 75% B was increased linearly to 90% B in 20 min, subsequently holding for 15 min, then raised to 95% B in10 min, and maintained for 20 min constantly; finally, eluent B reached 100% in 15 min and maintained for another 20 min. Initial conditions were reached in another 60 min.